Synthesis and Use of 3-Amino-4-phenyl-2-piperidones and 4-Amino-2-benzazepin-3-ones as Conformationally Restricted Phenylalanine Isosteres in Renin Inhibitors[1]

S. E. de Laszlo,* B. L. Bush,† J. J. Doyle, W. J. Greenlee, D. G. Hangauer, T. A. Halgren,† R. J. Lynch,‡ T. W. Schorn,‡ and P. K. S. Siegl‡

Departments of Exploratory Chemistry and Molecular Systems, Merck Sharp and Dohme Research Laboratories, Rahway, New Jersey 07065, and Department of Pharmacology, Merck Sharp and Dohme Research Laboratories, West Point, Pennsylvania 19486. *Received June 28, 1991*

The design of P_2-P_3 conformational restrictions in renin inhibitors by the use of a renin computer graphic model led to the synthesis of inhibitors containing *N*-Boc, *N*-acetyl, and *N*-phthalyl derivatives of 3(*S*)-amino-4(*R*,*S*)-2-piperidones and 4(*S*)-amino-2-benzazepinones in place of phenylalanine in the control compound *N*-acetyl-L-phenylalanyl-*N*-[4(*S*)-[(butylamino)carbonyl]-1(*S*)-(cyclohexylmethyl)-2(*S*)-hydroxy-5-methylhexyl]-L-norleucinamide (**32**). The piperidone inhibitors were prepared by utilization of the Evans chiral auxilliary to introduce the amino group with enantioselectivity and also to act as a leaving group in an intramolecular cyclization to the piperidone. The most potent inhibitor, 3(*S*)-(acetylamino)-α(*S*)-butyl-*N*-[4(*S*)-[(butylamino)carbonyl]-1(*S*)-(cyclohexylmethyl)-2(*S*)-hydroxy-5-methylhexyl]-2-oxo-4(*R*)-phenyl-1-piperidineacetamide (**18**, IC_{50} = 21 nM), was 25-fold less potent than the acyclic control **32**. Considerable dependence of potency with the size of the P_4 derivative was observed as had been expected based on the presynthetic modeling studies. Attempts to rationalize the observed potencies on the basis of further molecular modeling studies suggested that the loss in inhibitor potency was due to the conformational restrictions distorting the 3*S* center from the geometry present in the putative extended conformation present when the inhibitor is bound within the renin active site.

Introduction

Inhibition of the aspartyl protease renin as a therapeutic strategy for controlling hypertension is a goal that has stimulated much research in recent years.[2] Renin is the first enzyme in the renin angiotensin system (RAS), a metabolic cascade which results in the formation of the potent vasoconstricting hormone angiotensin II (AII) (Scheme I). Effective means exist for mediating RAS through the inhibition of angiotensin converting enzyme (ACE).[3] ACE is responsible for processing the decapeptide angiotensin I (AI) to the octapeptide angiotensin II (AII). ACE is not specific for AI alone, but also cleaves kinins and other endogenous peptides; thus its inhibition has the potential for side effects. The cleavage of angiotensinogen to give AI is catalyzed by renin and is the first and rate-limiting step in the formation of AII. Renin, in contrast to ACE, is a highly specific enzyme with angiotensinogen as its only known substrate. For this reason inhibition of renin may prove to be a preferred method of controlling the formation of AII.

Most inhibitors of renin developed to date are based on either substrate analogues or transition-state mimics of the P_1-P_1' scissile bond, extended with the minimum number of peptide residues or analogues thereof necessary for good potency.[4] The potential utility of peptide-based compounds as orally efficacious renin inhibitors is compromised by poor bioavailability. This is due to negligible oral absorption, susceptibility to enzymatic cleavage within the gut and vasculature, and secretion into the bile, all probable consequences of the high molecular weight and peptidic nature of renin inhibitors developed to date.[2] The introduction of conformational restrictions into a drug may improve potency by reducing the loss of entropy that occurs on its binding to a drug receptor or enzyme active site. This increased potency may in turn permit the use of fewer amino acid residues and thereby lower molecular weight and improve bioavailability. The use of conformationally restricted amino acid surrogates within peptide-based inhibitors may increase metabolic stability and enhance oral absorption.[5] The specificity of the inhibitor may be enhanced by excluding conformations amenable to inhibiting other enzymes.

Presynthetic Modeling of Conformationally Restricted Inhibitors

The Merck human renin binding site model was utilized to design three classes of P_2-P_3 conformationally restricted renin inhibitors, as follows.[6] We began with the crystallographically determined conformation of an acyclic renin inhibitor, L-363,564 (Figure 2),[7] as determined by

† Department of Molecular Systems.
‡ Department of Pharmacology.

(1) A portion of this work has appeared in preliminary form: de Laszlo, S. E.; Bush, B. L.; Doyle, J. J.; Greenlee, W. J.; Hangauer, D. G.; Halgren, T. A.; Lynch, R. J.; Schorn, T. W.; Siegl, P. K. *Peptides: Chemistry, Structure, and Biology Proceedings of the Eleventh American Peptide Symposium*: Rivier, J. E., Marshall, G. R., Eds.; ESCOM: Leiden, 1990; p 409-410.

(2) Greenlee, W. J. Renin Inhibitors. *Med. Res. Rev.* **1990**, *10*, 173-236.

(3) Wyvratt, M. J.; Patchett, A. A. Recent Developments in the Design of Angiotensin-Converting Enzyme Inhibitors. *Med. Res. Rev.* **1985**, *5*, 483-531.

(4) Schechter, I.; Berger, A. On the Size of the Active Site in Proteases. I. Papain. *Biochem. Biophys. Res. Commun.* **1961**, *27*, 157-162.

(5) Luly, J. R.; Fung, A. K. L.; Plattner, J. J.; Marcotte, P. A.; BaMaung, N.; Soderquist, J. L.; Stein, H. H. *Peptides, Chemistry and Biology. Proceedings of the Tenth American Peptide Symposium*; Marshall, G., Ed., ESCOM Science Publishers, B. V.: Leiden, 1988, p 487. Williams, P. D.; Perlow, D. S.; Payne, L. S.; Holloway, M. K.; Siegl, P. K. S.; Scorn, T. W.; Lynch, R. J.; Doyle, J. J.; Strouse, J. F.; Vlasuk, G. P.; Hoogsteen, K.; Springer, J. P.; Bush, B. L.; Halgren, T. A.; Richards, A. D.; Kay, J.; Veber, D. F. Renin Inhibitors Containing Conformationally Restricted P_1-P_1' Dipeptide Mimetics. *J. Med. Chem.* **1991**, *34*, 887-900.

(6) Bush, B. L.; Halgren, T. A. Unpublished results. For details of the model see the experimental section.

(7) L-363,564 (Boc-His-Pro-Phe-His-Sta-Leu-PheNH$_2$): Boger, J.; Lohr, N. S.; Ulm, E. H.; Poe, M.; Blaine, E. H.; Fanelli, G. M.; Lin, T.-Y.; Payne, L. S.; Schorn, T. W.; Lamont, B. I.; Vassil, T. C.; Stabilito, I. I.; Veber, D. F.; Rich, D. H.; Bopari, A. S. Novel Renin Inhibitors Containing the Amino Acid Statine. *Nature* **1983**, *303*, 81-84. (Compound IV.)

0022-2623/92/1835-0833$03.00/0

Scheme I. Renin Angiotensin System

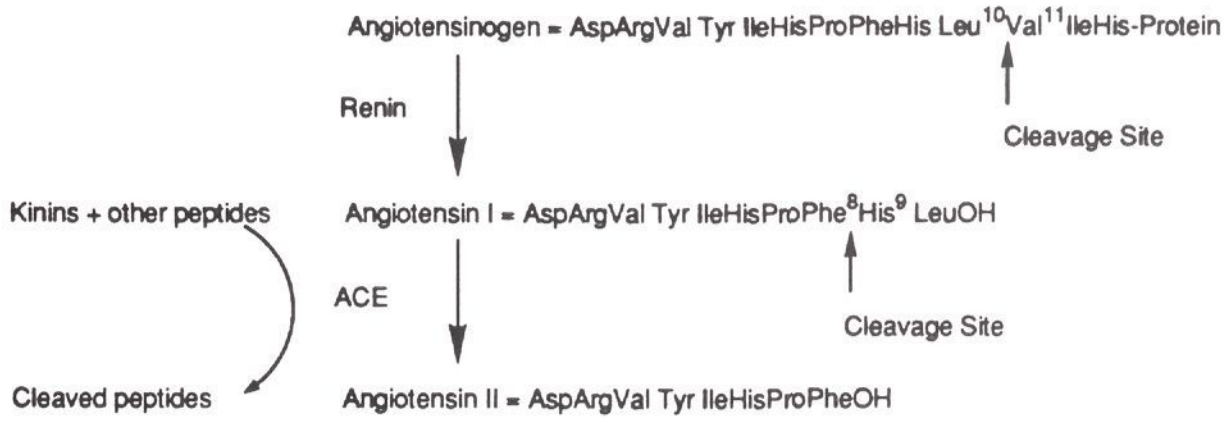

Figure 1. Renin binding model (blue), showing for clarity only residues within 9 Å of the P_3 α-carbon. Model of L-363,564 (yellow), with P_6 Boc at upper right. Models AF1, BF1, common portion white; P_4 Boc of BF1, purple.

Foundling et al. in the aspartyl protease endothiapepsin.[8] This conformation, which we denote EL0, was energetically relaxed into the renin binding site model to give the conformation EL1 (Figure 1).[9] Thaisrivongs et al. had shown that superior potency in P_2 N-alkylated analogues was elicited by a hydroxyethylene isostere at the renin cleavage point rather than the statine residue used in L-363,564.[10]

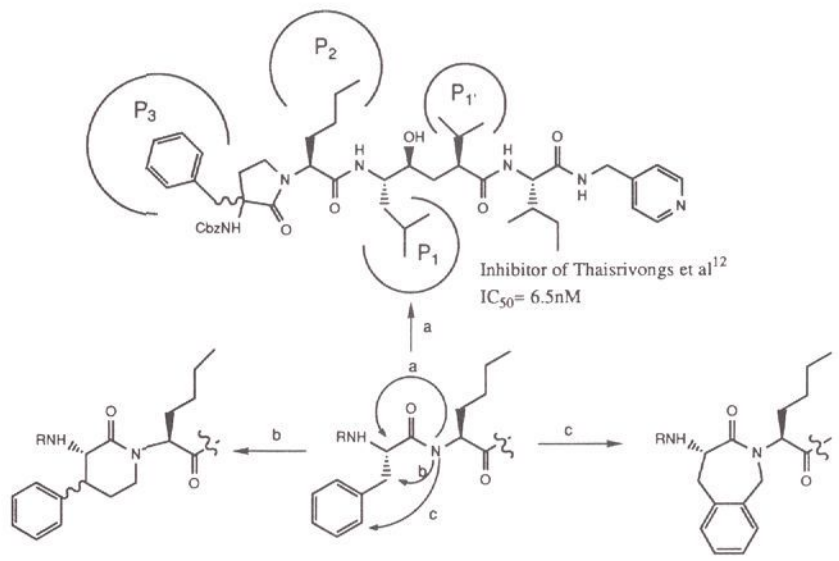

Figure 2. P_2-P_3 lactams as conformational restriction of phenylalanine.

We modified EL1 by introducing the hydroxyethylene isostere homo-ACHPA as the P_1-P_1' unit and norleucine in place of the histidine side chain in order to simplify the

(8) (a) Foundling, S. I.; Cooper, J.; Watson, F. E.; Cleasby, A.; Pearl, L. H.; Sibanda, B. L.; Hemmings, A.; Wood, S. P.; Blundell, T. L.; Valler, M. J.; Norey, C. G.; Kay, J.; Boger, J.; Dunn, B. M.; Leckie, B. J.; Jones, D. M.; Atrash, B.; Hallett, A.; Szelke, M. High Resolution X-ray Analyses of Renin Inhibitor–Aspartic Proteinase Complexes. *Nature* **1987**, *327*, 349–352. (b) Cooper, J. B.; Foundling, S. I.; Jupp, R. A.; Kay, J.; Blundell, T. L.; Boger, J. X-ray Studies of Aspartic Proteinase-Statine Inhibitor Complexes. *Biochemistry* **1989**, *28*, 8596–8603. Coordinates courtesy of Prof. T. L. Blundell (private communication).

(9) We designate conformations by an abbreviated name for the compound, followed by a single digit code denoting the conformation (see Table I). Abbrevation EL refers to the endothiapepsin-bound conformation of inhibitor L-363,564. Compounds modeled for this study are denoted AB and BB for *N*-acetyl and *N*-t-Boc benzazepinones, respectively, APR and BPR for *N*-acetyl and *N*-*t*-Boc (4*R*)-piperidones, APS and BPS for the corresponding (4*S*)-piperidones.

(10) Thaisrivongs, S.; Pals, D. T.; Harris, D. W.; Kati, W. M.; Turner, S. R. Design and Synthesis of a Potent and Specific Renin Inhibitor with a Prolonged Duration of Action. *J. Med. Chem.* **1986**, *29*, 2088–2093.

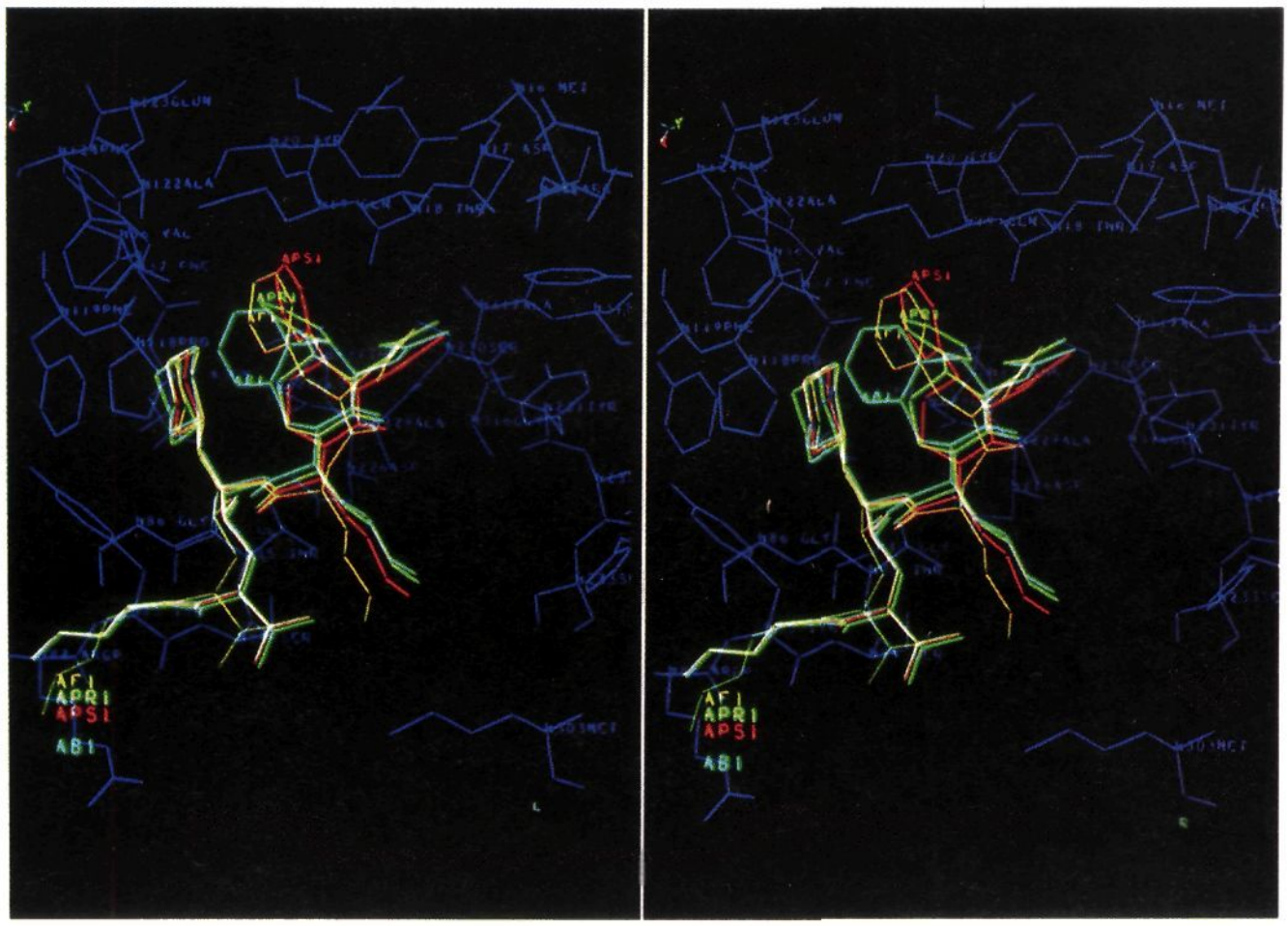

Figure 3. Initial P_4 acetyl models in renin binding model (blue): AF1 (yellow), piperidones APR1 (green), APS1 (red), benzazepinone AB1 (light blue).

chemistry.[11] The amino acid residues at P_4-P_7 were replaced with *N*-acetyl or *N*-*t*-Boc at P_4. All replacements were initially positioned by analogy with EL1. The inhibitor conformations were then energetically relaxed into the rigid enzyme model, generating the two models, AF1 and BF1, illustrated in Figure 1.

Inspection of the P_2-P_3 region of these models suggested that three conformational restrictions may be introduced (illustrated in Figure 2) which would not unduly perturb the overall conformation. Molecular models of the desired restrictions were constructed for the γ-lactams (cyclization "a"), the 2-piperidones (cyclization "b"), and the benzazepinones (cyclization "c"). Since a greater number of bonds become fixed into a particular conformation as one proceeds from cyclization "a" to "c", the magnitude of the potential benefit from the restricitions increases, as does the chance of error. Of the three cyclizations, "a" seemed to be best tolerated within the model active site and the least risky. While this work was in progress, Thaisrivongs reported the cyclized inhibitor **1** (Figure 1) with an IC_{50} = 6.5 nM, a 4-fold improvement over the corresponding acyclic inhibitor.[12] We were encouraged by these results to investigate cyclizations "b" and "c" in the hope of further improvements in potency and additional understanding of the renin active site topography.

It was assumed that the *S* absolute configuration would be maintained at the P_3 α-carbon by conformational analogy with L-phenylalanine in the acyclic compounds. The absolute configuration of the phenyl-bearing methine (C4) of the piperidones was modeled in both *S* and *R* configurations, since it was unclear which might provide a better overlay with the phenylalanine side chain of the acyclic models. The conformational restrictions were modeled by introducing the required carbon atoms and bonds into the acyclic model AF1, adjusting atomic positions locally to idealize the bond lengths and angles around the new rings, and then fully energy-optimizing the conformation. Each piperidone diastereomer also has two alternate ring puckers to be considered. The two alternative ring puckers were built for each diastereomer and were energy-minimized within the active site, then their binding modes were compared to that of the acyclic inhibitor. The unmodified portions of the structure moved only slightly during this exercise. A good overlay was found between one pucker of the 4*S* diasteromer and the acyclic model and a moderately good overlay for one 4*R* pucker and the acyclic model. Figure 3 illustrates the resulting overlay of the acyclic model AF1, the best puckers of the *N*-acetyl-(*S*)- and -(*R*)-piperidones (APS1, APR1; cyclization "b"), and the *N*-acetylbenzazepinone (AB1 cyclization "c"). The associated conformational data for these models and the Boc analogues appear in Table I. The main chains of all the models retained close similarity to the acyclic models, in particular retaining good hydrogen bonds to the P_3 CO from Ser 230 NH, and from P_3 NH to Ser 230 alcohol. The phenyl of the 4*S* compound lay close to the expected position in the S_3 pocket; in the 4*R* compound, it occupied an unexpected "slot" close to the well-defined second catalytic loop (renin residue 228) and terminated by the main chain of residue His 18 and the side chain of Gln 19. Although with care both piperidone configurations could be built without steric conflict with the enzyme, the models indicated that the phenyl of the (4*S*)-piperidones would give a superior overlay on the phenyl side chain of the acyclic model, implying that the (4*S*)-piperidones were more suitable than the 4*R* compounds as conformationally restricted analogues.

The modeling was repeated for the *N*-Boc derivatives and the inhibitor structures were compared to that found for the *N*-acetyl analogues as illustrated in Figure 3. It

(11) HACHPA or homo-ACHPA is (2*S*,4*S*,5*S*)-5-(*N*-Boc-amino)-6-cyclohexyl-4-hydroxy-2-isopropylhexanoic acid. Buhlmeyer, P.; Caselli, A.; Fuhrer, W.; Goshke, R.; Rasetti, V.; Rueger, H.; Stanton, J. L.; Criscione, L.; Wood, J. M. Synthesis and Biological Activity of Some Transition-State Inhibitors of Human Renin. *J. Med. Chem.* **1988**, *31*, 1839–1846.

(12) Thaisrivongs, S.; Pals, D. T.; Turner, S. R.; Kroll, L. T. Conformationally Constrained Renin Inhibitory Peptides: γ-Lactam-Bridged Dipeptide Isostere as Conformational Restriction. *J. Med. Chem* . **1988**, *31*, 1369–1376.

Table I. Geometric Parameters of Inhibitor Models

A. Main-Chain Torsion Angles (ϕ, ψ, ω) (deg)[a]

residue	P_4	P_3	P_2	P_1	P_1'	P_2'
			Compound L-363, 564 (ref 5)			
EL0	−57, 164, 179	−132, 137, 174	−141, 83, −174	−115, 61, −	78, 120, 174	−90, −165, 180
EL1	−104, 156, 177	−113, 146, 148	−137, 136, −166	−144, 64, −	68, 146, −169	−113, 152, −175
EL2	−84, 165, −178	−117, 148, 147	−137, 135, −166	−143, 64, −	68, 146, −169	−113, 152, −176
			Compound **32**			
AF1	−, −, −172	−121, 163, 147	−129, 123, 178	−116, 55, 143	−70, 131, 173	
AF2	−, −, −171	−114, 115, −176	148, 128, 179	−116, 56, 146	−74, 136, 173	
			Compound **31**			
BF1	−168, 171, −161	−122, 165, 146	−127, 122, 178	−115, 55, 143	−70, 131, 173	
BF2	−169, 171, −168	−99, 125, −170	−148, 127, 178	−115, 56, 146	−74, 135, 173	
			Compound **18**			
APR1	−, −, 177	−147, −178, −175	−168, 190, −177	−125, 52, 147	−63, 112, −167	
APR2	−, −, −151	37, −110, 163	−139, 105, −178	−121, 51, 145	−64, 118, −170	
APR3	−, −, −176	96, −137, 156	−140, 75, 170	−111, 64, 130	−64, 130, 176	
			Compound **17a**			
BPR1	−179, 177, 178	−157, −179, −175	−173, 108, −170	−125, 53, 146	−58, 110, −167	
BPR2	49, −136, −160	51, −90, 150	−153, 85, 177	−104, 63, 141	−54, 132, −176	
BPR3	102, 167, 176	3, −101, 155	−156, 78, 179	−107, 67, 139	−59, 136, 178	
BPR4	49, −170, 180	−129, −90, 150	−153, 85, 177	−104, 63, 141	−54, 133, −176	
BPR6	64, 140, −163	39, −102, 167	−152, 108, −174	−126, 55, 145	−62, 117, −168	
			Compound APS[b]			
APS1	−, −, −172	−138, 174, 178	−162, 106, −178	−115, 50, 148	−64, 115, −169	
APS2	−, −, −159	−176, −68, 177	−161, 101, −176	−118, 50, 150	−64, 121, −172	
APS3	−, −, −153	37, −112, 163	−136, 104, 179	−120, 51, 145	−64, 117, −169	
APS4	−, −, −165	78, −117, 154	−147, 97, −176	−120, 57, 139	−65, 123, 177	
			Compound **17b**			
BPS1	−179, 158, −156	−120, 167, −178	−167, 106, −178	−115, 50, 149	−64, 115, −170	
BPS2	100, 143, −152	179, −101, −165	−140, 111, −165	−128, 51, 149	−63, 121, −172	
BPS3	63, 138, −161	38, −102, 170	−152, 108, −174	−126, 55, 145	−62, 116, −168	
BPS4	79, 131, −170	57, −121, 164	−150, 101, −168	−125, 57, 141	−64, 123, 178	
BPS5	79, 131, 180	−133, −121, 164	−150, 101, −168	−125, 57, 141	−64, 123, 178	
			Compound **28**			
AB1	−, −, −177	−151, 169, −173	−165, 116, −173	−131, 49, 148	−64, 116, −170	
AB2	−, −, −171	141, −74, 174	−156, 113, −177	−119, 53, 151	−69, 136, −180	
AB3	−, −, 174	−147, 166, −169	−176, 98, −147	−132, 52, 158	−69, 144, 177	
			Compound **27**			
BB1	−163, 147, −140	−112, 163, −172	−168, 116, −177	−129, 49, 148	−64, 116, −169	
BB2	73, 164, −151	149, −27, 146	−74, 144, −176	119, 56, 150	−68, 142, 176	
BB3	−163, 163, −160	−121, 162, −168	−178, 100, −149	−131, 52, 158	−69, 144, 177	

B. Side-Chain Torsion Angles and P_3 Cyclic Torsion Angles (deg)[d]

residue	P_3	P_3 ring	P_2	P_1	P_1'
		Compound L-363,564			
EL0	−73, 91	−	168, 28	−51, 169	−
EL1	−67, 91	−	179, 20	−61, 167	−
EL2	−66, 90	−	179, 20	−61, 167	−
		Compound **32**			
AF1	−61, 110	−	−177, 179, 173	−56, 166	168
AF2	−48, 108	−	−180, 174, 174	−53, 168	165
		Compound **31**			
BF1	−59, 108	−	−176, 179, 173	−56, 166	168
BF2	−46, 107	−	−179, 175, 175	−53, 168	166
		Compound **18**			
APR1	76, 1	−8, 45, −21, −33, 68, −50	−135, −171, 180	−54, 166	179
APR2	−48, −92	−6, 20, −48, 58, −47, 21	−122, −174, 180	−49, 162	178
APR3	57, −147	−33, −4, 50, −54, 20, 24	−112, −173, 179	−53, 174	180
		Compound **17a**			
BPR1	80, 7	−9, 47, −23, −31, 67, −49	174, 173, 178	−58, 169	179
BPR2	−48, −100	−30, 24, −30, 42, −49, 44	175, 167, 178	−51, 163	179
BPR3	27, 123	−44, 12, 38, −53, 24, 25	177, 162, 178	−57, 171	179
BPR4	−48, −101	−30, 42, −48, 44, −49, 44	175, 162, 178	−50, 163	179
BPR6	−42, −88	−21, 33, −51, 56, −46, 28	180, 172, 170	−51, 167	177
		Compound APS			
APS1	−72, −43	20, 41, −61, 16, 40, −64	−142, −171, −175	−52, 165	178
APS2	−179, 173	−30, 27, −43, 59, −65, 52	−133, −174, −177	−52, 165	178
APS3	−149, 146	−4, 18, −46, 58, −45, 19	−125, −172, 180	−48, 163	178
APS4	−83, 119	−8, −36, 69, −55, 15, 19	−121, −175, 180	−51, 163	176

Table I (Continued)

B. Side-Chain Torsion Angles and P_3 Cyclic Torsion Angles (deg)[d]

residue	P_3	P_3 ring	P_2	P_1	P_1'
		Compound 17b			
BPS1	-66, -30	23, 39, -60, 16, 41, -66	-146, -169, -172	-52, 166	176
BPS2	-167, 170	1, 10, -46, 67, -57, 24	174, 169, 180	-52, 162	178
BPS3	-146, 143	-22, 31, -49, 54, -45, 29	180, 172, 180	-51, 168	178
BPS4	-75, 101	-1, -40, 69, -57, 21, 10	180, 169, 179	-53, 163	178
BPS5	-75, 101	-1, -40, 69, -57, 21, 10	180, 169, 179	-53, 163	178
		Compound 28			
AB1	-140, 138	-15, 58, -18, -7, -37, 96, -69	-130, -172, 180	-53, 159	178
AB2	48, -149	20, -72, 36, 2, 28, -81, 61	-162, -175, 173	-51, 163	172
AB3	-148, 142	-7, 52, -27, -2, -35, 90, -72	176, 167, -179	-140, 168	173
		Compound 27			
BB1	-140, 142	-11, 59, -21, -8, -33, -71	-131, -172, -178	-53, 159	178
BB2	-53, -160	-39, -31, 38, -3, 18, -69, 98	-179, -177, 176	-55, 164	171
BB3	-146, 145	-4, 57, -30, -1, -33, 89, -75	175, 165, -179	-141, 169	173

[a] Torsion angles listed for acyclic peptide residues (or Pro) are ϕ, ψ, ω, as defined by IUPAC convention. For other residues, analogous torsion angles are listed; the third (ω), when listed, is always a C(O)–N amide torsion. For cyclic P_3 residues the ψ and ω torsions are referred to extracyclic atoms (P_3 N and P_2 Cα, respectively). For P_4 Boc, the torsions listed are those about C–O, O–C(O), and C(O)–N; for P_4 Ac, the single torsion is about C(O)–N. Statline and or homo-ACHPA are notated as a dipeptide analogue -P_1-P_1'-, so that the P_1 torsions are N–C, C–C(OH), and C(OH)–C (the last omitted in Sta); the P_1' torsions are C–C, C–C(O), and C(O)–N. [b] Compound not synthesized. Notation for compounds and conformations is described in footnote 6 of the text. [c] Reference 9, compound ~VIa,b of Table I. The stereoisomer chosen for the lactam 2 position corresponds to naturally occurring L-phenylalanine. The Cbz group defines an additional torsional angle not present in the other compounds; its value is -75°. [d] Torsion angles for acyclic side chains are χ_1, χ_2, defined by IUPAC convention. The analogous angles are indicated for the phenyl substituent on P_3 piperidones. Ring torsion angles for the P_3 lactam rings are indicated beginning with the C(O)–N lactam bond and proceeding toward N.

was found that the bulky Boc group moved upon energy minimization due to a steric interaction with the enzyme active site whereas the acetyl group was readily accommodated. The remaining portions of the inhibitor did not move substantially from that of the corresponding acyclic inhibitor. The steric crowding suggested that cyclic inhibitors with an N-acetyl terminus on the P_3 residue would be more active than an *N*-Boc terminus.

These exploratory modeling results were promising enough to encourage us to design and carry out the synthesis of these compounds and of acyclic controls.

Chemistry

The synthesis of the 3(*S*)-amino-4(*RS*)-phenyl-2-piperidones illustrated as APS1 and APR1 (Figure 3) depends on the successful enantioselective construction of a 3,4-disubstituted piperidone ring system (Scheme II). Commercially available 3-phenylglutaric acid was dehydrated with DCC to give anhydride **2** which was reduced with $NaBH_4$ to lactone **3** following the protocol of Bailey and Johnson in 81% overall yield.[13] The lactone was saponified and esterified to ester **4** in 35% yield. Swern oxidation of the alcohol and immediate protection of the aldehyde as the dioxolane gave **5** in 80% yield. It should be mentioned that initial attempts at completing this synthesis with alcohol **4** protected as the TBDMS ether were frustrated by the difficulties we encountered in its deprotection later in the synthetic route (vide infra). Ester **5** was saponified to give acid **6** in 93% yield. The pivaloyl anhydride of **6** was treated with the lithium salt of (*S*)-4-benzyl-2-oxazolidinone following the protocol of Evans to give a mixture of two diastereotopic imides **7a** and **7b** in 80% yield.[14] These imides were readily separable by chromatography, the less polar being **7a** and the more polar **7b**. The imides were converted to the azides **8a** and **8b**, respectively, by treatment of their potassium enolates with triisopropylbenzenesulfonyl azide as described by Evans (98% and 65% yields).[15] Inspection of the ^1H NMR spectra of these diastereomeric azides indicated that they were at least 95% enantiomerically pure. Hydrolysis of the acetal function followed. Surprisingly vigorous conditions (3:1:1 $CH_3COOH/H_2O/THF$, 95 °C, 6 h) were necessary to achieve this conversion to aldehydes **9a** and **9b** in 67% and 79% yields, respectively. Use of a TBDMS-protected alcohol in place of an acetal failed to give reliably reproducible yields of the desired primary alcohol on deprotection, the balance of the deprotection reaction mixture consisting of products derived from lactonization with concomitant loss of the oxazolidinone. For this reason, oxidation to the aldehyde oxidation state was carried out at an earlier step in the synthesis in the expectation that the aldehyde could be reliably revealed without complicating side reactions later in the sequence. However, a sample of azide **10** derived from the silyl ether sequence was crystallized from CH_2Cl_2/hexanes and its X-ray structure was determined (Figure 4). The known C4-*S* configuration of the oxazolidinone determined that the absolute configuration at C2 and C3 were *S* and *R*, respectively. The C3-*S* diastereomer of **10** was converted to aldehyde **9b** by silyl ether hydrolysis followed by Swern oxidation. This material was found to be identical to aldehyde **9b** derived from the acetal route. Since the Evans technology introduces the azide with the same absolute configuration in both series as dictated by the chiral auxiliary, **9a** may be assigned as C2-*S*, C3-*R* and **9b** as C2-*S*, C3-*S*.

Reductive alkylation of **9a** with L-norleucine *tert*-butyl ester gave rise to a 55% yield of amine **11**. On heating **11** to 110 °C in DMF an 84% yield of piperidone **12a** could be isolated. When aldehyde **9b** was reductively alkylated

(13) Bailey, D. M.; Johnson, R. E. Reduction of Cyclic Anhydrides with $NaBH_4$. Versatile Lactone Synthesis. *J. Org. Chem.* **1970**, *35*, 3574–3576.

(14) Evans, D. A.; Weber, A. E. Asymmetric Glycine Enolate Aldol Reaction: Synthesis of Cyclosporine's Unusual Amino Acid, MeBmt. *J. Am. Chem. Soc.* **1986**, *108*, 6757–6761.

(15) Evans, D. A.; Britton, T. C. Electrophilic Azide Transfer to Chiral Enolates. A General Approach to the Asymmetric Synthesis of α-Amino Acids. *J. Am. Chem. Soc.* **1987**, *109*, 6881–6883.

Scheme II.[a] Synthesis of the 3(*S*)-Amino-4(*R,S*)-phenylpiperidones

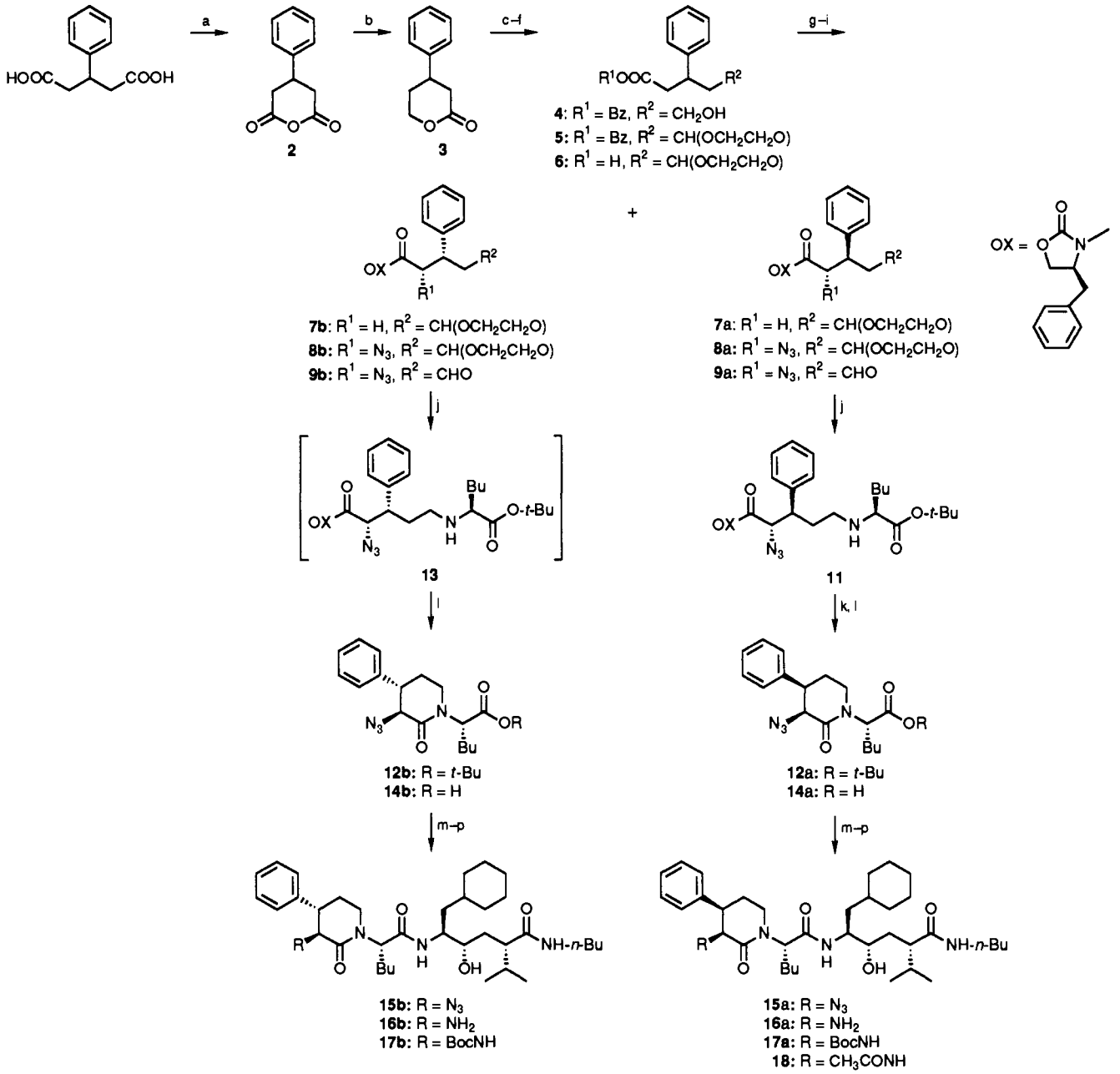

[a] (a) DCC, CH_2Cl_2, 95%; (b) $NaBH_4$, THF, H^+, 86%; (c) NaOH, H_2O; HMPA, $PhCH_2Br$, 57%; (d,e) Swern oxidation, $HOCH_2CH_2OH$, TsOH, PhH, 80%; (f) NaOH, THF, H_2O, 93%; (g) *t*-BuCOCl, Et_3N, −78 °C; (*S*)-(−)-4-benzyl-2-oxazolidinone, BuLi, −78 °C, 80%, 1:1 mixture; (h) $KN(TMS)_2$, THF, $TrisN_3$, −78 °C, 98% (**13a**), 65% (**13b**); (i) HOAc, H_2O, THF, 90 °C, 67% (**14a**), 79% (**14b**); (j) $NaCNBH_4$, MeOH, 3-Å sieves, 55% (**16**), 38% (**17b**); (k) DMF, 110 °C, 84%; (l) HCl, EtOAc, 100%; (m) NH_2HACHPA-NH-*n*-Bu, DMEC, HOBt, CH_2Cl_2, 0 °C, 50% (**19a**), 60% (**19b**); (n) $HSCH_2CH_2SH$, Et_3N, MeOH, 57%; (o) Boc_2O, CH_2Cl_2, 80%; (p) $(CH_3CO)_2O$, Et_3N, 70%.

under the same conditions as in the case of **9a**, no amine was isolated, but a 38% yield of piperidone **12b** was formed. This result suggests that intermediate amine **13** is formed and spontaneously cyclizes under the conditions of the reaction. The difference in behavior of **9a** and **9b** is a consequence of the greater steric crowding evident in the transition state formed in the cyclization of amine **11** over that of **13**. Inspection of the ^1H NMR spectra of **12a** and **12b** indicated that no detectable racemization had taken place.

The two piperidone *tert*-butyl esters **12a** and **12b** were hydrolyzed by treatment with saturated HCl in EtOAc to give acids **14a** and **14b**. The acids were coupled under standard conditions to (2*S*,4*S*,5*S*)-5-amino-6-cyclohexyl-4-hydroxy-2-isopropylhexanoic acid to give peptides **15a** and **15b**.[16] The azide functionality was reduced to the primary amines **16a** and **16b**. The amines were converted to the Boc derivatives **17a** and **17b** by treatment with Boc_2O. Amine **16a** was further N-acylated with acetic anhydride to give acetamide **18**.

The synthesis of chiral 3-aminobenzazepin-2-one as illustrated as AB1 in Figure 3 could be approached from three retrosynthetic bond disconnections (Scheme III). In approach "α" the seven-membered ring could be prepared from the formation of an amide bond from the amino acid precursor shown. If bond "β" is broken the ring system

(16) Chakravarty, P. K.; de Laszlo, S. E.; Sarnella, C. S.; Springer, J. P.; Schuda, P. F. The Synthesis of (2*S*,4*S*,5*S*)-5-(*N*-Boc)-amino-6-cyclohexyl-4-hydroxy-2-isopropyl-hexanoic acid Lactone, an Hydroxyethylene Dipeptide Isostere Precursor. *Tetrahedron Lett.* **1989**, *30*, 415–418.

Table II. Potency and Analysis of Renin Inhibitors

	IC_{50}, nM	analysis	EIMS exact mass calcd	EIMS exact mass found	FABMS	t_R[b]
17a	134	$C_{41}H_{68}N_4O_6 \cdot 0.3H_2O$		*a*	713	5.99
17b	5910	$C_{41}H_{68}N_4O_6 \cdot 0.25H_2O$		*a*	713	5.38
18	21	$C_{38}H_{61}N_4O_5$[a]	654.4720	654.4722	655	4.76
25	>20000	$C_{43}H_{60}N_4O_6 \cdot 0.7H_2O$	728.4513	728.4511	729	5.97
26	2040	$C_{35}H_{58}N_4O_4 \cdot 0.6H_2O$	598.4458	598.4439	599	4.56
27	1730	$C_{40}H_{66}N_4O_6 \cdot 0.2H_2O$	698.4982	698.4984	699	5.77
28	210	$C_{38}H_{61}N_4O_5$[a]	640.4564	640.4566	641	4.86
29	87	$C_{42}H_{60}N_4O_6 \cdot 0.8H_2O$	716.4513	716.4511	717	5.65
31	2.1	$C_{39}H_{66}N_4O_6$[a]		*a*	687	*a*
32	0.84	$C_{36}H_{60}N_4O_5$[a]	628.4563	628.4534	629	4.31

[a] Analysis not carried out. [b] t_R = retention time during HPLC with 85% CH_3CN/H_2O/0.1% trifluoroacetic acid at 0.75 mL/min, a Dynamax C_{18} (4.5 mm × 25 cm) column, and detection at 254 nM.

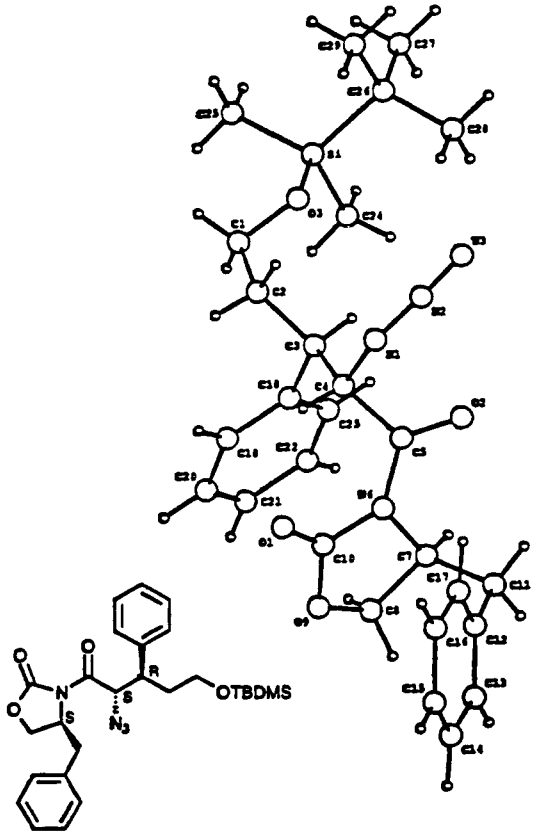

Figure 4. X-ray crystallographic structure of **10**.

could be seen as being derived from the intramolecular alkylation of an amide by a benzylic leaving group. Lastly, "γ", the formation of a iminium cation, could lead to the benzazepine ring by an intramolecular Pictet–Spengler type of ring closure.[17] We attempted all of these synthetic approaches. In support of approaches α and β, the racemic precursor **19** was prepared. Appropriate functional-group modifications and condensations with norleucine via either acylation with the carboxylic acid of **19** or reductive alkylation of a benzaldehyde formed from **19** gave the required precursors. Unfortunately all attempts at forming bond α and β failed.

A simple and highly efficient method of forming the benzazepin-2-one ring system was found by forming bond γ in the key step (Scheme IV).[17] L-*N*-Phthalylphenylalaninyl-L-norleucine methyl ester (**21**) was prepared by conventional amino acid condensation. The ester was hydrolyzed to acid **22** and condensed with formaldehyde to give chiral oxazolone **23**. No detectable racemization

(17) Flynn, G. A. European Patent Application 0 249 223, 1987.

Scheme III. Retrosynthetic Examination of Benzazepinone Synthesis

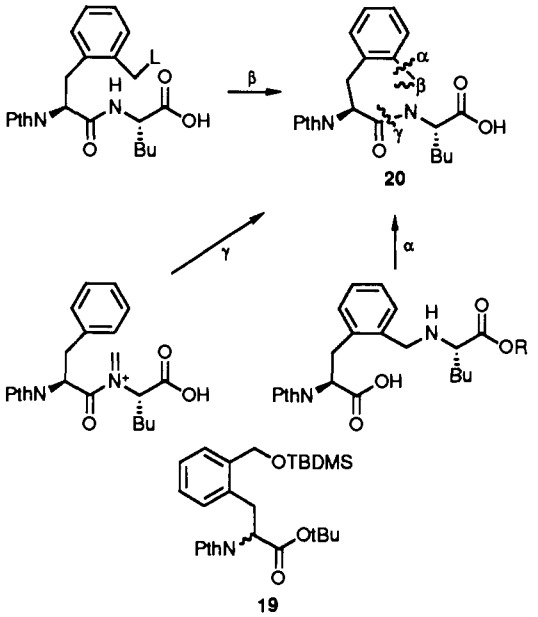

had occurred at either of the two chiral centers during these transformations as measured by ^1H NMR. When oxazolone **23** was treated with triflic acid in CH_2Cl_2 at room temperature, very high yields (96%) of 3-aminobenzazepin-2-one **24** was isolated. The remarkable efficiency of this process was reflected in its selectivity with approximately 10% racemization occurring at one of the chiral centers (as measured by detection of an additional diastereomer formed in the cyclization by ^1H NMR). Acid **24** was condensed with amine (2*S*,4*S*,5*S*)-5-amino-6-cyclohexyl-4-hydroxy-2-isopropylhexanoic acid to give peptide **25**. The phthaloyl protecting group was removed to give amine **26**. The amine was acylated under standard conditions to give rise to the *N*-Boc and *N*-acetyl peptides **27** and **28**.

The control inhibitors were prepared in the usual manner (Scheme IV). L-*N*-Phthaloylphenylalaninyl-L-norleucine (**22**) was condensed under standard conditions with (2*S*,4*S*,5*S*)-5-amino-6-cyclohexyl-4-hydroxy-2-isopropylhexanoic acid to give inhibitor **29**. The phthaloyl protecting group was removed to give rise to amine **30**. Acylation with Boc_2O and acetic anhydride gave *N*-Boc and *N*-acetyl derivatives **31** and **32**.

Results and Discussion

The compounds listed in Table II were assayed as inhibitors of human plasma renin at pH 7.4 with IC_{50}'s as shown. The acyclic control compounds **29**, **31**, and **32** were all potent inhibitors of renin as was expected from the

Scheme IV. Synthesis of Benzazepinone and Control Inhibitors of Renin

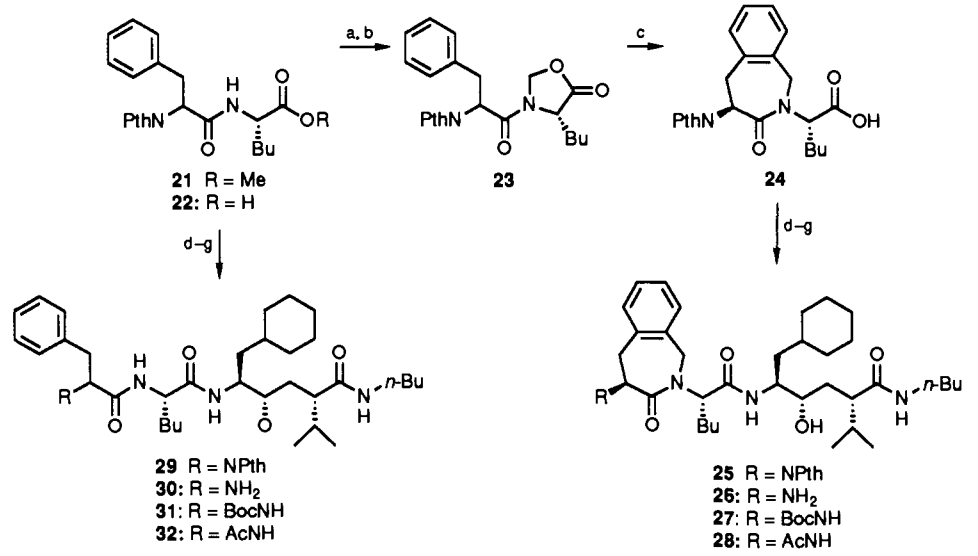

[a] (a) acetone, HCl, H_2O, 60%; (b) $(CH_2O)_n$, TsOH, PhH, Dean–Stark trap, 63%; (c) CF_3SO_3H, CH_2Cl_2, 96% (10% racemization); (d) NH_2-HACHPA-NH-*n*-Bu, DMEC, HOBt, CH_2Cl_2, 0 °C, 78%; (e) NH_2NH_2, EtOH, reflux, 94%; (f) Boc_2O, Et_3N, CH_2Cl_2, 86%; (g) $(CH_3CO)_2O$, Et_3N, CH_2Cl_2, 100%.

potencies reported for similar acyclic inhibitors based on the hydroxyethylene isostere. The potency of the acyclic inhibitors was sensitive to the P_4 acyl group: the *N*-phthalyl and *N*-Boc derivatives **29** and **31** are 100 and 2.5 times less potent than **32**, which bears the smaller *N*-acetyl group. This result suggested that the potency of inhibitors would be sensitive to any changes which would affect the preferred placement of P_4 with respect to P_3 and was experimentally supported by the reduction of inhibitory potency on introduction of either the benzazepinone or the piperidone conformational restriction. The most potent of the conformationally restricted inhibitors were the *N*-Boc- and *N*-acetyl-(3*S*,4*R*)-piperidones **17a** and **18**, which were, respectively, 65 and 25 times less potent than controls **31** and **32**. (3*S*,4*S*)-Piperidone **17b** was approximately 40 times less potent than the 3*S*,4*R* isomer **17a**. The benzazepinone-based inhibitors **25–28** were between 250 and 1000 times less potent than the controls. *N*-Boc analogue **27** was equipotent with the free amine **26**. Within this series, the *N*-acetyl analogue was approximately 10-fold more potent than the *N*-Boc and the amino analogues **27** and **26**.

The presynthetic modeling studies had suggested that *N*-acetyl derivatives of the cyclic inhibitors would be more potent than the more bulky *N*-Boc derivatives. This prediction was supported by the experimental results in all three series: the acyclic controls (**31** and **32**), the (4*R*)-piperidones (**17a** and **18**), and the benzazepinones (**27** and **28**). The degree of improvement in potency from replacing Boc with acetyl was much greater in the cyclic series than the acyclic controls. This had been predicted in the presynthetic modeling studies.

We had expected that the (4*S*)-piperidones would be more potent than the (4*R*)-piperidones based on the overlay observed for the best of the two (4*S*)-piperidone puckers examined. The 25-fold reduction in potency of (4*R*)-piperidone **18** when compared to acyclic control **32** corresponds to a reduction of binding energy of approximately 1.8 kcal/mol.[18] The fact that **18** binds as well as it does when compared to the control suggested that aspects of our energy-relaxed model of the inhibitor binding conformation did not reflect the actual binding geometry. Consequently, we carried out additional molecular modeling studies of the phenylalanine isosteres by approaching the model construction through an alternative approach to see whether alternative low-energy conformations might be found. The Cambridge Crystallographic Data Base[19] was searched for 2-piperidone and benzazepin-3-one ring fragments using the Cambridge program QUEST.[20] The limited information available on 2-piperidinones was supplemented by geometries of analogous cyclohexenes. In the absence of crystal information on benzazepinones, we compiled structures of benzo-fused cycloheptenes and of (1,4)-cycloheptadienes. The consensus conformation for the piperidones is a half-chair; its torsion angles, listed in the same order as in Table I, are −3°, 18°, −48°, 63°, −49°, 19°. This is distinctly different from the envelope conformations found in the extended models described in the presynthetic modeling. The consensus for benzazepinones has torsion angles of about −7°, 77°, −57°, 1°, −4°, 58°, −67°. As a check of this consensus, 30–100 distinct conformations of each ring were generated by distance–geometry methods and energy-optimized; in each case, the global minimum conformation agreed within 2°–3° of that listed above. Each consensus structure was reflected through the ring plane to yield a second starting geometry.

The P_4 group and P_3 side chain appropriate to each compound were attached and the resulting fragments were linked into model AF1 through the P_2 α-carbon. In all cases the P_3 carbonyl was assumed to continue to form a hydrogen bond with the renin backbone. (We note that Thaisrivongs et al. advance the possibility that γ-lactams lacking a P_4 residue may bind with the lactam reversed, sacrificing this hydrogen bond in order to keep the P_3

(18) Note: the corresponding 4(*S*)-acetylpiperidone diastereomer of **18** was not prepared due to the large increase in potency elicited by **17a** over **17b**.

(19) Allen, F. H.; Bellard, S. A.; Brice, M. D.; Cartwright, B. A.; Doubleday, A.; Higgs, H.; Hummelink, T.; Hummelink-Peters, B. G.; Kennard, O.; Motherwell, W. D. S.; Rodgers, J. R.; Watson, D. G. The Cambridge Crystallographic Data Center: Computer-based Search, Retrieval, Analysis and Display of Information. *Acta Crystallogr.* **1979**, *B35*, 2331–2339.

(20) Program QUEST89: Cambridge Crystallographic Data Center, Software Development, Lensfield Road, Cambridge, CB2 1EW, U.K.

phenyl group positioned in the conventional S_3 pocket.) For the larger ring structures considered here, however, such reversed binding is highly unlikely on steric grounds. The rotational possibilities of the P_4 group were manually surveyed within the renin site model. Finally, the best inhibitor conformations were energy-minimized by the stepwise procedure described in the Experimental Section, to insure that the model would adjust to the binding site with minimum distortion of the specified ring pucker and rotamer.

The resulting models (BPR2-4 and -6, BPS2-5, APR2-4, APS2-5, AB2-3, BB2-3) are described in Table I. These conformations were examined when docked within the renin model and compared against the acyclic controls and the initial models APS1, APR1, and AB1. Although all models attained geometries which were free of gross steric overlap, each cyclic model possessed qualitative weaknesses when compared to the acyclic compounds. In most models, the ring geometry is substantially distorted—the result of accomodating a steric conflict between the ring substituents and the renin binding site or the P_1 cyclohexyl ring of the inhibitor itself. Where this is not the case, the phenyl projects directly into solution where it would sacrifice hydrophobic binding.

In retrospect, the observed loss in potency of the conformationally restricted inhibitors when compared to the controls was seen to result from a single cause: distortion of the 3*S* center because of conflicting geometric requirements from lactamizing through the P_3 side chain and yet maintaining an extended conformation of the P_4-P_3 main chain. Lactamization through the P_3 side chain must distort the extended conformation of the P_4-P_3 main chain. Lactamization through the P_3 side chain must distort the extended conformation of the peptide backbone. In the case of the γ-lactams prepared by Thaisrivongs, the extended conformation of the peptide backbone may be maintained without loss of the approximate spatial position of the P_3 and P_4 groups by cyclizing the *pro-R* hydrogen of the P_3 center with the amide P_2 hydrogen. These hydrogen atoms are syn to each other in an extended conformation; thus linking them with a 2-carbon bridge is not damaging to the overall conformation.

The improved potency of the *N*-acetyl analogues over the *N*-Boc analogues is a reflection of the reduced steric conflicts that result from the conformational restrictions forcing the P_4 substituent out of its conventional S_4 binding site.

The renin model used herein may be called into question. Sielecki has reported the X-ray crystal structure of recombinant human renin but atomic coordinates have not been reported.[21] We have compared the renin model against the crystal structures of three groups of porcine pepsin, recently deposited in the Protein Data Bank by three laboratories.[22] All residue α-carbons of the model involved with contacts with the P_3-P_4 conformations described here lie within 1.5 Å of their counterparts in pepsin and the side chains of the model project in similar direction to their analogues in pepsin. Thus we believe that the renin model is sufficiently accurate for the qualitative modeling that has been carried out in this work.

Conclusions

Molecular modeling was used to design conformationally restricted analogues of phenylalanine in the P_3 site of renin inhibitors. The enantioselective synthesis of 3-amino-4-phenylpiperidones and the 3-aminobenzazepinones was accomplished and the resulting heterocycles were introduced into renin inhibitors containing a hydroxyethylene isostere at the scissile bond. The inhibitory potencies of these compounds were determined and compared to that of control compounds. The observed reduction in potency resulting from the introduction of the conformational restrictions was then investigated by further molecular modeling.

The molecular modeling studies and the biological data give support for an extended conformational geometry of renin inhibitors at the P_3-P_4 region. These studies also indicate that potency losses due to unfavorable enzyme/inhibitor binding interactions may be compensated by the introduction of smaller groups at proximal positions. These results support increased effort in the design and preparation of other conformationally restricted renin inhibitors. The more we understand about the binding mode of renin inhibitors, the more likely the opportunity will arise to design a potent nonpeptidic renin inhibitor.

ICI has reported the use of P_4-P_3 amino acid replacements which bear no resemblance to the Pro-Phe region of the natural substrate.[23] This approach in combination with the development of conformationally restricted mimetics and the structure of enzyme inhibitor complexes may in the future lead to greater understanding of how renin inhibitors bind within the active site.

Experimental Section

Modeling Studies. A model of the three-dimensional structure of human renin was built using the crystallographic modeling program FRODO,[24] based upon crystal structures of the three fungal aspartyl proteases: rhizopuspepsin,[25] endothiapepsin,[26] and penicillopepsin.[27] Following the guidelines described by Greer[28] (see ref 29 for a more recent discussion) the main chains of the

(21) Sielecki, A. R.; Hayakawa, K.; Fujinaga, M.; Murphy, M. E. P.; Fraser, M.; Muir, A. K.; Carilli, C. T.; Lewicki, J. A.; Baxter, J. D.; James, M. N. G. Structure of Recombinant Human Renin, a Target for Cardiovascular-Active Drugs, at 2.5 Å Resolution. *Science* **1989**, *243*, 1346–1349.

(22) (a) Abad-Zapatero, C.; Erickson, J. W. Brookhaven Protein Data Bank entry 3PEP. (b) Andreeva, N.; Fedorov, A. A.; Sielecki, A.; James, M. Brookhaven Protein Data Bank entry 4PEP. (c) Cooper, J. B.; Khan, G.; Taylor, G.; Tickle, I. J.; Blundell, T. L. Brookhaven Protein Data Bank entry 5PEP. (d) Brookhaven Protein Data Bank: Bernstein, F. C.; Koetzle, T. F.; Williams, G. J. B.; Meyer, E. F., Jr.; Brice, M. D.; Rodgers, J. R.; Kennard, O.; Shimanouchi, T.; Tasumi, M. The Protein Data Bank: A Computer-based Archival File for Macromolecular Structures. *J. Mol. Biol.* **1977**, *112*, 535–542.

(23) Roberts, D. A.; Bradbury, R. H.; Brown, D.; Faull, A.; Griffiths, D.; Major, J. S.; Oldham, A. A.; Pearce, R. J.; Ratcliffe, A. H.; Revill, J.; Waterson, D. 1,2,4-Triazolo[4,3-*a*]pyrazine Derivatives with Human Renin Inhibitory Activity. 1. Synthesis and Biological Properties of Alkyl Alcohol and Statine Derivatives. *J. Med. Chem.* **1990**, *33*, 2326–2334.

(24) Jones, T. A. A Graphics Model Building and Refinement System for Macromolecules. *J. Appl. Crystallogr.* **1978**, *11*, 268–272.

(25) Suguna, K.; Bott, R. R.; Padlan, E. A.; Subramanian, E.; Sheriff, S.; Cohen, G. H.; Davies, D. R. Structure and Refinement at 1.8 Å Resolution of the Aspartic Proteinase from Rhizopus Chinensis. *J. Mol. Biol.* **1987**, *196*, 877–900. Coordinates: Brookhaven Protein Data Bank entry 2APR.

(26) Blundell, T. J.; Jenkins, J. A.; Sewell, B. T.; Pearl, L. H.; Cooper, J. B.; Tickle, I. J.; Veerapandian, B.; Wood, S. P. The Three-dimensional Structure at 2.1 Å Resolution of Endothiapepsin. *J. Mol. Biol.* **1990**, *211*, 919–941. Coordinates: Brookhaven Protein Data Bank entry 4APE.

(27) James, M. N. G.; Sielecki, A. R. Structure and Refinement of Penicillopepsin at 1.8 Å Resolution. *J. Mol. Biol.* **1983**, *163*, 299–361. Coordinates: Brookhaven Protein Data Bank entry 2APP.

(28) Greer, J. Comparative Model-Building of the Mammalian Serine Proteases. *J. Mol. Biol.* **1981**, *153*, 1027–1042.

protein crystal structures were first superimposed to identify the conserved framework. We then took this structural information into account in aligning sequences and in modeling the features specific to renin (side-chain conformations and nonconserved loops). FRODO option "REFI" was used extensively to produce reasonable covalent geometry, and nonbonded contacts and main-chain dihedrals were monitored throughout the process.

From the full renin model, a smaller binding site model was then constructed for inhibitor docking studies. Crystal structures of extended inhibitors H-142 and L-363,564 complexed to endothiapepsin (coordinates, private communication from Prof. T. L. Blundell) were used to define starting conformations for inhibitor models, and to identify enzyme residues surrounding the binding cleft.[5] The resulting binding site model consists of 94 residues. Numbered according to the renin sequence, with pepsin sequence numbers in parentheses where the correspondence is unambiguous, they are 13–21 (7–20), 36–45 (30–39), 80–88 (72–80), 118–131 (111–124), 134–137 (127–130), 198–202 (187–191), 224–233 (213–221), 252–254, 286–290, and 297–321 (283–308). Titratable residues are charged except for neutral Asp 17, Asp 226, Glu 288, Arg 321, and His 301 (protonated ND1). Because this model was left rigid for the modeling reported here, the positioning of side chains and the flexible "flap" was crucial. Ser 230, Ser 84, and Thr 85 were modeled to preserve the network of hydrogen bonds described by Szelke et al.[5] The Gln 19 side chain was placed to allow maximum room for an aromatic P_3 group. Except for these choices, most aspects of this renin model which bear on the modeling described were clearly guided by homology with the fungal enzymes. The coordinates of the resulting renin binding site model are available as supplementary material.

Computer models of the compounds were created, using the facilities of the Merck modeling systems MOLEDIT[30] and its successor system AMF, and visually superposed on the reference structure using FRODO.

All conformations described in this article were energy-relaxed within the renin binding site model, using an extended version of the MM2 force field[31] as implemented by the OPTIMOL program within MOLEDIT or AMF. A dielectric constant of 1.5 was employed; no "solvent-screened" or "distant-dependent" electrostatic model was used. Except as noted, geometries reported in Table I were optimized to a gradient of 0.04 kcal/mol per Å or less.

The stepwise procedure for relaxing each model in the renin active site was as follows. Ring models were constructed by energy optimization, using the consensus values of cyclic torsion angles as restraints. Amide bonds were also restrained to planarity. Initial energy relaxation was used to repair nonideal bonded geometry and intramolecular collisions. After the intramolecular energy had been reduced to approximately 100 kcal/mol or less, the interactions with the enzyme model were introduced gradually, with scaling to avoid energies greater than approximately 1000 kcal/mol, and 50 cycles of optimization were carried out at a time while the interaction scale with the enzyme was increased. When necessary, optimization was first performed with torsions only, to keep the bonded geometry intact and allow for wide excursions of the rotatable groups. After all unfavorable interactions with the enzyme had been relieved, the restraints were removed and the ring systems fully optimized.

General Procedures. All reactions were carried out under an atmosphere of dry nitrogen gas unless noted otherwise. Solvents used in reactions were anhydrous as supplied by Aldrich. THF was dried over sodium and benzophenone and distilled freshly before use. Thin-layer chromatography was carried out on E. Merck silica 60 F_{254} plates eluting with the solvent noted in the experimental details. Medium-pressure chromatography was carried out over E. Merck Lobar silica 60 columns of the size noted utilizing a refractive index and UV detector at 254 nm. E. Merck silica gel (230–400 mesh) was used for flash chromatography. NMR spectra were measured on a Varian XL 300-MHz spectrometer. Elemental analysis were within 0.4% of calculated values and were measured at MSDRL.

3-Phenylglutaric Anhydride (2). To a suspension of 25 g (120 mmol) of 3-phenylglutaric acid in 200 mL of CH_2Cl_2 at 0 °C was added 26 g (126 mmol) of dicyclohexylcarbodiimide in 100 mL of CH_2Cl_2. After stirring overnight and allowing the temperature to rise to room temperature, the suspension was diluted with 200 mL of hexanes and filtered. The filtrate was concentrated in vacuo and the residue recrystallized from a mixture of 80 mL of EtOAc and 100 mL of hexanes to give **2** as colorless crystals: 21.8 g (114 mmol), 95% yield; mp 140–142 °C; ^{1}H NMR ($CDCl_3$) δ 2.87 (dd, 2 H, J = 11.6, 16.3 Hz), 3.12 (ddd, 2 H, J = 4.4, 16.6, 1 Hz), 3.43 (m, 1 H), 7.19–7.48 (m, 5 H). Anal. ($C_{11}H_{10}O_3$) C, H.

3-Phenyl-δ-valerolactone (3). To a suspension of 0.97 g (25.6 mmol) of $NaBH_4$ in 20 mL of dry THF at 0 °C was added a solution of 4.89 g (26 mmol) of anhydride **2** in 20 mL of dry THF under N_2. The solution was stirred at 0 °C for 1 h, and was then warmed to room temperature for 0.5 h. To this solution was added 10 mL of 6 M HCl at 0 °C dropwise. The solution was concentrated in vacuo. The residue was redissolved in 100 mL of toluene in the presence of a catalytic amount of *p*-TsOH and concentrated to dryness. This procedure was repeated twice. The product was Kugelrohr distilled to give a colorless oil: 3.9 g (22 mmol), 86% yield; bp 165–170 °C (1 mmHg); ^{1}H NMR ($CDCl_3$) δ 1.92–2.08 (m, 1 H), 2.09–2.18 (m, 1 H), 2.60 (dd, 1 H), 2.88 (dd, 1 H), 3.20 (m, 1 H), 4.40 (m, 2 H), 7.15–7.38 (m, 5 H).

Benzyl 5-Hydroxy-3-phenylpentanoate (4). To 3.4 g (19.4 mmol) of lactone **3** was added 8.5 mL of a 2.5 M solution of NaOH in water. The reaction mixture was stirred overnight and concentrated in vacuo. The residue, dissolved in 250 mL of 4:1 toluene/MeOH, was concentrated to dryness. This procedure was repeated to give rise to 4.08 g (19.4 mmol) of the dry sodium salt. To a suspension of the salt in a mixture of 10 mL of HMPA/2 mL of EtOH was added 3.65 g (21 mmol) of benzyl bromide at room temperature. The reaction mixture was stirred overnight, diluted with 100 mL of ether, and partitioned with 50 mL of water. The aqueous phase was extraced with ether (2 × 50 mL). The combined ethereal phases were washed with water (4 × 50 mL) and saturated NaCl (1 × 50 mL) and dried over $MgSO_4$. The residue following filtration and concentration was purified by MPLC chromatography (Lobar C column, SiO_2, 35% EtOAc/hexane) to give 3.08 g (11.1 mmol) of a colorless oil: 57% yield; ^{1}H NMR ($CDCl_3$) δ 1.89 (m, 2 H), 2.70 (m, 2 H), 3.32 (m, 1 H), 3.50 (bm, 2 H), 5.02 (s, 2 H), 7.17–7.40 (m, 10 H).

Benzyl 4-(1,3-Dioxolan-2-yl)-3-phenylbutanoate (5). To a solution of 1.5 g (11.7 mmol) of oxalyl chloride in 70 mL of dry CH_2Cl_2 at −78 °C was added 2.14 g (27.5 mmol) of dry DMSO. After stirring for 15 min, a solution of 2.97 g (11 mmol) of alcohol **4** in 10 mL of CH_2Cl_2 was added dropwise followed after 0.5 h by 5.55 g (55 mmol) of Et_3N. The suspension was allowed to warm to room temperature and was diluted with 200 mL of ether and washed with water (3 × 10 mL) and saturated NaCl (1 × 20 mL) and was dried over $MgSO_4$. After filtration and concentration of the filtrate in vacuo, the residue (2.94 g) was dissolved in 50 mL of benzene to which was added 0.83 g (13.3 mmol) of ethylene glycol and a catalytic amount of TsOH. The reaction mixture was heated under a Dean–Stark trap at 120 °C for 2 h. The reaction mixture was concentrated in vacuo to 5 mL (Note: the intermediate aldehyde and product **5** have the same R_f in 30% EtOAc/hexane) and the residue filtered through a pad of silica gel. The filtrate was purified following concentration by MPLC (Lobar C column, 20% EtOAc/hexane) to give a colorless oil: 2.80 g (8.88 mmol), 80% yield; ^{1}H NMR ($CDCl_3$) δ 1.9–2.1 (m, 2 H), 2.6–2.85 (m, 2 H), 3.42 (m, 1 H), 3.75 (m, 2 H), 3.92 (m, 2 H), 4.63 (dd, 1 H, J = 3.4, 6.7 Hz), 5.02 (s, 2 H), 7.17–7.40 (m, 10 H); FABMS m/z 327 (M^+ + 1). Anal. ($C_{20}H_{22}O_4$) C, H.

4-(1,3-Dioxolan-2-yl)-3-phenylbutanoic Acid (6). A solution of 2.70 g (8.4 mmol) of ester **5** in 25 mL of THF and 8.7 mL of

(29) Greer, J. Comparative Modeling Methods: Application to the Family of Serine Proteases. *Proteins: Struct., Func., Genet.* **1990**, *7*, 317–334.

(30) (a) Gund, P.; Andose, J. D.; Rhodes, J. B.; Smith, G. M. Three-dimensional Molecular Modeling and Drug Design. *Science* **1980**, *208*, 1425–1431. (b) Smith, G. M.; Hangauer, D. G.; Andose, J. D.; Bush, B. L.; Fluder, E. M.; Gund, P.; McIntyre, E. F. Intermolecular Modeling Methods in Drug Design/Modeling the Mechanism of Peptide Cleavage by Thermolysin. *Drug. Inf. J.* **1984**, *18*, 167–178.

(31) (a) Burkert, U.; Allinger, N. L. *Molecular Mechanics*; ACS Monograph 177; American Chemical Society: Washington, DC, 1982. (b) Allinger, N. L. Conformational Analysis. 130. MM2. A Hydrocarbon Force Field Utilizing V1 and V2 Torsional Terms. *J. Am. Chem. Soc.* **1977**, *99*, 8127–8134.

1 M NaOH was refluxed for 10 h. The solution was diluted with 15 mL of water, extracted with ether (3 × 5 mL), and acidified to pH 2.0. The aqueous phase was then extracted with ether (3 × 10 mL). The combined ethereal extracts were washed with saturated NaCl (1 × 10 mL) and dried over $MgSO_4$, filtered, and concentrated in vacuo to give a white crystalline solid: 1.77 g (7.5 mmol), 93% yield; mp 104–106 °C; ^1H NMR ($CDCl_3$) δ 1.9–2.1 (m, 2 H), 2.64 and 2.78 (AB dd, 2 H, J = 8.3, 15.8 Hz), 3.37 (m, 1 H), 3.75 (m, 2 H), 3.92 (m, 2 H), 4.62 (dd, 1 H, J = 3.4, 6.7 Hz), 7.18–7.35 (m, 5 H), COOH, not observed; EIMS m/z 236 (M^+). Anal. ($C_{13}H_{16}O_4$) C, H.

3-[4-(1,3-Dioxolan-2-yl)-1-oxo-3(*R*)-phenylbutyl]-4(*S*)-(phenylmethyl)-2-oxazolidinone (7b). 3-[4-(1,3-Dioxolan-2-yl)-1-oxo-3(*S*)-phenylbutyl]-4(*S*)-(phenylmethyl)-2-oxazolidinone (7a). A solution of 1.19 g (5.0 mmol) of **6** in 5.0 mL of dry THF at −78 °C was treated with 0.55 g (5.5 mmol) of Et_3N followed by 0.63 g (5.5 mmol) of pivaloyl chloride. In a separate flask 0.93 g (5.25 mmol) of (*S*)-(−)-4-benzyl-2-oxazolidinone was dissolved in 13 mL of dry THF and was cooled to −78 °C. To this solution was added 2.1 mL of a 2.5 M solution of *n*-butyllithium in hexanes (5.25 mmol). After stirring for 10 min the solution was added via cannula to the suspension of the acid anhydride. The mixture was stirred at −78 °C for 10 min and then warmed to 0 °C for 0.5 h. The reaction mixture was partitioned between 50 mL of EtOAc and 50 mL of water. The aqueous phase was extracted with EtOAc (3 × 25 mL), and the combined organic phases were washed with saturated $NaHCO_3$ solution (2 × 10 mL) and dried over $MgSO_4$. The solution was filtered and concentrated in vacuo. The residue was purified by MPLC (Lobar C column, 35% EtOAc/hexane) to give two fractions.

Less polar fraction (**7a**): 0.78 g (1.9 mmol), 40% yield; mp 111–113 °C; ^1H NMR ($CDCl_3$) δ 1.95–2.18 (m, 2 H), 2.67 (dd, 1 H, J = 6.8, 7.5 Hz), 3.18–3.22 (m, 2 H), 3.39–3.58 (m, 2 H), 3.78 (m, 2 H), 3.90–4.09 (m, 4 H), 4.50 (m, 1 H), 4.68 (dd, 1 H, J = 3.4, 6.8 Hz), 7.12–7.38 (m, 10 H); FABMS m/z 396 ($M^+ + 1$). Anal. ($C_{23}H_{25}NO_5$) C, H, N.

More polar fraction (**7b**): 0.78 g (1.9 mmol), 40% yield; mp 86–87 °C; ^1H NMR ($CDCl_3$) δ 1.95–2.18 (m, 2 H), 2.54 (dd, 1 H, J = 13.5, 9.16 Hz), 2.98 (dd, 1 H, J = 3.4, 13.6 Hz), 3.20 (m, 1 H), 3.53 (m, 2 H), 3.38 (m, 2 H), 3.93 (m, 2 H), 4.10 (m, 2 H), 4.58–4.71 (m, 2 H), 7.0 (m, 2 H), 7.18–7.40 (m, 8 H); FABMS 396 ($M^+ + 1$). Anal. ($C_{23}H_{25}NO_5$) C, H, N.

3-[4-(1,3-Dioxolan-2-yl)-1-oxo-3(*S*)-phenyl-2(*S*)-azidobutyl]-4(*S*)-(phenylmethyl)-2-oxazolidinone (8b). 3-[4-(1,3-Dioxolan-2-yl)-1-oxo-3(*R*)-phenyl-2(*S*)-azidobutyl]-4(*S*)-(phenylmethyl)-2-oxazolidinone (8a). To a solution of 4.04 mL (2.0 mmol) of 0.5 M potassium hexamethyldisilazide in toluene dissolved in 4 mL of dry THF at −78 °C was added a precooled −78 °C solution of 0.73 g (1.8 mmol) of imide **7a** or **7b** in 8.0 mL of THF via a cannula. The reaction mixture was stirred for 0.5 h. A precooled solution of 0.7 g (2.26 mmol) of 2,4,6-triisopropylbenzenesulfonyl azide in 4 mL of THF was added via a cannula. The reaction mixture was stirred for 3 min, at which time was added 0.5 mL of acetic acid (8.2 mmol). The solution was warmed to 35 °C for 0.5 h. The reaction mixture was diluted with 50 mL of EtOAc and partitioned with 20 mL of saturated NaCl solution. The organic phase was washed with saturated $NaHCO_3$ solution (2 × 20 mL) and dried over $MgSO_4$. Following filtration and concentration, the residue was purified as indicated below.

8a: Flash chromatography over silica gel (30% EtOAc/hexane) gave 0.78 g of an oil (98% yield); ^1H NMR ($CDCl_3$) δ 2.28 (m, 2 H), 2.68 (dd, 1 H, J = 10.1, 12.3 Hz), 3.20 (dd, 1 H, J = 2.1, 12.5 Hz), 3.38–3.53 (m, 2 H), 3.77 (m, 2 H), 3.92 (m, 3 H), 4.10 (m, 1 H), 4.64 (t, 1 H, J = 3.8 Hz), 5.26 (d, 1 H, J = 9.8 Hz), 7.12–7.38 (m, 10 H); FABMS m/z 436 ($M^+ + 1$). Anal. ($C_{23}H_{24}N_4O_5$) C, H, N.

8b: The reaction was carried out as above, and purification by MPLC on a Lobar C silica column (50% EtOAc/hexane) gave a 65% yield of a colorless solid; mp 79–81 °C; ^1H NMR ($CDCl_3$) δ 1.90 (m, 1 H), 2.20 (m, 1 H), 2.85 (dd, 1 H, J = 13.7, 9.7 Hz), 3.30 (dd, 1 H, J = 13.5, 3.3 Hz), 3.52 (m, 1 H), 3.75 (m, 2 H), 3.92 (m, 2 H), 4.25 (m, 2 H), 4.55–4.70 (m, 2 H), 5.51 (d, 1 H, J = 8.8 Hz), 7.2–7.4 (m, 10 H). FABMS m/z 436 ($M^+ + 1$). Anal. ($C_{23}H_{24}N_4O_5$) C, H, N.

3-[2(*S*)-Azido-1,5-dioxo-3(*S*)-phenylpentyl]-4(*S*)-(phenylmethyl)-2-oxazolidinone (9b). 3-[2(*S*)-Azido-1,5-dioxo-3(*R*)-phenylpentyl]-4(*S*)-phenylmethyl-2-oxazolidinone (9a). A solution of 0.76 g (1.74 mmol) of acetal **8a** or **8b** in a mixture of 3 mL of acetic acid, 1 mL of THF, and 1 mL of water was heated at 90 °C for 6 h and then at room temperature overnight. The reaction mixture was concentrated in vacuo and the residue redissolved in EtOAc and washed with saturated $NaHCO_3$, water, and brine. The solution was dried over $MgSO_4$, filtered, and concentrated. Flash chromatography of the residue over silica gel eluting with 30% EtOAc/hexane gave a single product as indicated below.

9a: 0.46 g (1.17 mmol), 67% yield; ^1H NMR ($CDCl_3$) δ 2.76 (dd, 1 H, J = 9.7, 13.5 Hz), 2.93 (ddd, 1 H, J = 1, 6.9, 18.4 Hz), 3.23 (dt, 2 H, J = 12.6, 5.3 Hz), 3.84–3.96 (m, 2 H), 4.07 (dd, 1 H, J = 2.1, 8.9 Hz), 4.28 (m, 1 H), 5.42 (d, 1 H, J = 9.6 Hz), 7.22–7.38 (m, 10 H), 9.72 (s, 1 H). Anal. ($C_{21}H_{20}N_4O_4 \cdot 0.25H_2O$) C, H, N.

9b: 79% yield; ^1H NMR ($CDCl_3$) δ 2.78–2.89 (m, 3 H), 2.98 (dd, 1 H, J = 1.7, 8.57 Hz), 3.27 (dd, 1 H, J = 3.2, 13.4 Hz), 3.88 (dt, 1 H, J = 5.8, 8.52 Hz), 4.22 (d, 1 H, 5.21 Hz), 4.59 (m, 1 H), 5.51 (d, 1 H, J = 8.57 Hz), 7.19–7.40 (m, 10 H), 9.61 (t, 1 H, J = 1.79 Hz). Anal. ($C_{21}H_{20}N_4O_4 \cdot 0.25H_2O$) C, H, N.

***N*-[4(*S*)-Azido-5-oxo-5-[2-oxo-4(*S*)-(phenylmethyl)-3-oxazolidinyl]-3(*R*)-phenylpentyl]-L-norleucine 1,1-Dimethylethyl Ester (11).** To a solution of 0.1 g (0.25 mmol) of aldehyde **9a** in 1 mL of dry MeOH was added 0.052 g (0.28 mmol) of L-norleucine *tert*-butyl ester followed by 150 mg of ground 3-Å molecular sieves. The reaction mixture was stirred for 0.5 h and then treated with 0.085 mL of a 1 M solution of $NaCNBH_4$ in THF. After stirring for 3 h at room temperature, the reaction mixture was filtered and the filtrate was concentrated in vacuo. The residue was dissolved in 20 mL of EtOAc, washed with water (3 × 7 mL) and saturated NaCl (1 × 10 mL), and dried over $MgSO_4$. The solution was filtered and concentrated in vacuo. The residue was purified by flash chromatography over silica, eluting with 20% EtOAc/hexanes to give a single major product as a glass: 78.9 mg (0.14 mmol), 55% yield; ^1H NMR ($CDCl_3$) δ 0.90 (m, 3 H), 1.25–1.37 (m, 4 H), 1.42 (s, 9 H), 1.40–1.79 (m, 4 H), 2.20 (m, 1 H), 2.33 (m, 1 H), 2.48 (m, 1 H), 2.68 (dd, 1 H, J = 9.76 Hz), 3.01 (t, 1 H, J = 6.62 Hz), 3.15–3.28 (m, 2 H), 3.45 (t, 1 H, J = 8.03 Hz), 3.92 (dd, 1 H, J = 1.9, 8.95 Hz), 4.05 (m, 1 H), 5.31 (d, 1 H, J = 9.93 Hz), 7.12–7.38 (m, 10 H); FABMS m/z 564 ($M^+ + 1$). Anal. ($C_{31}H_{41}N_5O_5$) C, H, N.

3(*S*)-Azido-α(*S*)-butyl-2-oxo-4(*R*)-phenyl-1-piperidineacetic Acid *tert*-Butyl Ester (12a). Amine 11 (0.065 g, 0.116 mmol) in 5 mL of dry DMF was heated at 110 °C for 5 h under N_2 until the starting material had been consumed and replaced by a less polar product (TLC 40% EtOAc/hexanes). The reaction mixture was concentrated in vacuo and the residue flash chromatographed over silica gel eluting with 15% EtOAc/hexane to give 37.5 mg (0.097 mmol) of piperidone **12a** (84% yield): ^1H NMR ($CDCl_3$) δ 0.94 (bt, 3 H), 1.25–1.55 (m, 4 H), 1.47 (s, 9 H), 1.74 (m, 1 H), 1.95–2.25 (m, 3 H), 2.85 (dt, 1 H, J = 3.79, 11.23 Hz), 3.28–3.46 (m, 2 H), 4.16 (d, 1 H, J = 10.7 Hz), 5.06 (dd, 1 H, J = 5.0, 10.7 Hz), 7.23–7.43 (m, 5 H); FABMS m/z 387 ($M^+ + 1$). Anal. ($C_{21}H_{30}N_4O_3$) C, H, N.

3(*S*)-Azido-α(*S*)-butyl-2-oxo-4(*S*)-phenyl-1-piperidineacetic Acid *tert*-Butyl Ester (12b). To a solution of 0.2 g (0.5 mmol) of aldehyde **9b** in 1 mL of dry MeOH was added 0.1 g (0.53 mmol) of norvaline *tert*-butyl ester and 200 mg of ground, activated 3-Å molecular sieves. After stirring for 1 h under N_2, 0.17 mL of a 1 M solution of $NaCNBH_4$ in THF was added. The reaction mixture was stirred for a further 2 h until all the starting material had been consumed. The mixture was filtered and the filtrate concentrated in vacuo. The residue was dissolved in 25 mL of EtOAc and 5 mL of water. The phases were separated and washed with water (2 × 10 mL) and saturated NaCl solution (1 × 10 mL). After drying over $MgSO_4$, the solution was filtered and concentrated. The residue was purified by flash chromatography eluting with 20% EtOAc/hexane to give 0.065 g (0.2 mmol) of piperidone **12b**: 38% yield; ^1H NMR ($CDCl_3$) δ 0.9 (t, 3 H), 1.2–1.52 (m, 4 H), 1.46 (s, 9 H), 1.69 (m, 1 H), 1.9–2.2 (m, 3 H), 2.94 (dd, 1 H, J = 3.7, 10.7 Hz), 3.24 (dt, 1 H, J = 4.5, 12.2 Hz), 3.41 (dd, 1 H, J = 4.4, 10.2 Hz), 4.17 (d, 1 H, J = 10.2), 5.10 (dd, 1 H, J = 5.3 Hz), 7.17–7.40 (m, 5 H); FABMS m/z 387 (M^+

+ 1). Anal. ($C_{21}H_{30}N_4O_3$) C, H, N.

3(*S*)-Azido-α(*S*)-butyl-*N*-[4(*S*)-[(butylamino)carbonyl]-1(*S*)-(cyclohexylmethyl)-2(*S*)-hydroxy-5-methylhexyl]-2-oxo-4(*R*)-phenyl-1-piperidineacetamide (15a). To a solution of 37.5 mg (0.1 mmol) of ester **12a** in 0.5 mL of EtOAc at room temperature was added 1.0 mL of EtOAc saturated with dry HCl. The solution was stirred overnight, concentrated in vacuo, the residue was dissolved in 10 mL of EtOAc and washed with water (2 × 3 mL) followed by brine (1 × 5 mL). The organic phase was dried over $MgSO_4$, filtered, and concentrated in vacuo to give 32 mg (0.1 mmol) of acid **14a**. The acid was dissolved in 1 mL of CH_2Cl_2 at 0 °C and treated with 32 mg (0.1 mmol) of the amine *N*-*n*-butyl-(2*S*,4*S*,5*S*)-5-amino-6-cyclohexyl-4-hydroxy-2-isopropylhexanamide, 16.3 mg (1.2 mmol) of *N*-hydroxybenzotriazole, and 23 mg (1.2 mmol) of 1-[3-(dimethylamino)propyl]-3-ethylcarbodiimide hydrochloride. The reaction mixture was stirred overnight at room temperature. The mixture was diluted with 20 mL of EtOAc and washed sequentially with saturated citric acid solution (2 × 5 mL), saturated $NaHCO_3$ solution (2 × 5 mL), and brine (1 × 5 mL). The organic phase was dried over $MgSO_4$ and filtered and the residue purified by flash chromatography over silica eluting with 95:5:0.01 $CHCl_3$/MeOH/NH_4OH to give 35.1 mg (0.05 mmol) of the desired peptide (R_f = 0.25) as a glass in 50% yield overall: characteristic ^1H NMR ($CDCl_3$) signals δ 2.83 (dt, 1 H, *J* = 3.9, 11.23 Hz), 4.09 (d, 1 H, *J* = 10.9 Hz), 4.98 (t, 1 H, *J* = 7.7 Hz), 5.89 (t, 1 H, *J* = 5.4 Hz), 6.45 (d, 1 H, *J* = 8.9 Hz), 7.19–7.41 (m, 5 H); EI exact mass calcd for $C_{36}H_{58}N_6O_4$ 638.4519, found 638.4520. HPLC t_R = 5.84 min, 85% CH_3CN/H_2O/0.1% TFA at 0.75 mL/min, Dynamax C_{18} (4.5 mm × 25 cm) column, detection at 210 nm.

3(*S*)-Azido-α(*S*)-butyl-*N*-[4(*S*)-[(butylamino)carbonyl]-1(*S*)-(cyclohexylmethyl)-2(*S*)-hydroxy-5-methylhexyl]-2-oxo-4(*S*)-phenyl-1-piperidineacetamide (15b). Following the protocol described for **15a**, ester **12b** was hydrolyzed and coupled to give crude peptide **15b**. The material was purified by MPLC on a Lobar A silica column eluting with 40% EtOAc/hexanes to give 40 mg (0.06 mmol) of peptide **15b** as a glass in 60% overall yield: characteristic ^1H NMR ($CDCl_3$) signals δ 2.89 (dt, 1 H, *J* = 4.2, 10.3 Hz), 3.52 (bd, 1 H, *J* = 10.7 Hz), 3.91 (bt, 1 H), 4.23 (d, 1 H, *J* = 9.9 Hz), 4.98 (t, 1 H, *J* = 7.71 Hz), 6.03 (7, 1 H, 5.8 Hz), 6.59 (d, 1 H, *J* = 9.3 Hz, 7.15–7.40 (m, 5 H); EI exact mass calcd for $C_{36}H_{58}N_6O_4$ 638.4519, found 638.4507; HPLC t_R = 5.65 min, 85% CH_3CN/H_2O/0.1% TFA at 0.75 mL/min, Dynamax C_{18} (4.5 mm × 25 cm) column, detection at 210 nm.

3(*S*)-Amino-α(*S*)-butyl-*N*-[4(*S*)-[(butylamino)carbonyl]-1(*S*)-(cyclohexylmethyl)-2(*S*)-hydroxy-5-methylhexyl]-2-oxo-4(*R*)-phenyl-1-piperidineacetamide (16a). 3(*S*)-Amino-α(*S*)-butyl-*N*-[4(*S*)-[(butylamino)carbonyl]-1(*S*)-(cyclohexylmethyl)-2(*S*)-hydroxy-5-methylhexyl]-2-oxo-4(*S*)-phenyl-1-piperidineacetamide (16b). Azido peptides **15a** and **15b** were both reduced in the following manner: To a solution of 18 mg (0.028 mmol) of **15a** or **15b** in 0.5 mL of degassed MeOH at room temperature was added 19.6 μL (0.14 mmol) of triethylamine and 13 μL (0.14 mmol) of ethanedithiol. The solution was stirred for 48 h and then concentrated in vacuo. The residue was purified by flash chromatography over silica eluting with EtOAc to give 10 mg (0.016 mmol) of amines **16a** and **16b** as glasses (57% yield).

16a: characteristic ^1H NMR ($CDCl_3$) signals δ 2.83 (bAB, 1 H, *J* = 4.66, 11.0 Hz), 3.55 (d, 1 H, *J* = 10.8 Hz), 3.62 (bt, 1 H, *J* = 4.3 Hz), 4.98 (t, 1 H, *J* = 7.76 Hz), 6.05 (t, 1 H, *J* = 5.4 Hz), 6.55 (d, 1 H, *J* = 9.3 Hz), 7.2–7.4 (m, 5 H); FABMS *m*/*z* 613 (M^+ + 1).

16b: characteristic ^1H NMR ($CDCl_3$) signals δ 2.84 (bAB, 1 H), 3.64 (d, 1 H, 10.7 Hz), 3.88 (bm, 1 H), 5.00 (t, 1 H, 7.81 Hz), 5.86 (t, 1 H, 5.75 Hz), 6.59 (d, 1 H, 8.9 Hz), 7.20–7.40 (m, 5 H); FABMS *m*/*z* 613 (M^+ + 1).

3(*S*)-[(*tert*-Butyloxycarbonyl)amino]-α(*S*)-butyl-*N*-[4-(*S*)-[(butylamino)carbonyl]-1(*S*)-(cyclohexylmethyl)-2-(*S*)-hydroxy-5-methylhexyl]-2-oxo-4(*R*)-phenyl-1-piperidineacetamide (17a). 3(*S*)-[(*tert*-Butyloxycarbonyl)amino]-α(*S*)-butyl-*N*-[4(*S*)-[(butylamino)carbonyl]-1(*S*)-(cyclohexylmethyl)-2(*S*)-hydroxy-5-methylhexyl]-2-oxo-4(*S*)-phenyl-1-piperidineacetamide (17b). Amines **16a** and **16b** were acylated with Boc_2O as follows: To a solution of 9 mg (0.015 mmol) of the amine in 0.5 mL of CH_2Cl_2 was added 10 mg (0.05 mmol) of di-*tert*-butyl dicarbonate. The solution was stirred overnight and concentrated in vacuo and the residue purified by flash chromatography over silica eluting with 50% EtOAc/hexane, to give 8.7 mg (0.012 mmol) of peptide **17a** or **17b** (80% yield) as glasses.

17a: characteristic ^1H NMR (CD_3OD) signals δ 1.31 (s, 9 H), 3.93 (m, 1 H), 4.10 (d, 1 H), 5.05 (t, 1 H), 7.2–7.35 (m, 5 H); FABMS *m*/*z* 713 (M^+ + 1). Anal. $C_{41}H_{68}N_4O_6 \cdot {}^1/_4H_2O$ C, H, N.

17b: characteristic ^1H NMR (CD_3OD) signals δ 1.31 (s, 9 H), 3.93 (bm, 1 H), 4.11 (bt, 1 H, *J* = 11.34 Hz), 5.03 (t, 1 H, *J* = 7.27 Hz), 6.89 (d, 1 H, *J* = 8.41 Hz), 7.20–7.35 (m, 5 H), 7.89 (bt, 1 H, *J* = 5.8 Hz); FABMS *m*/*z* 713 (M^+ + 1).

3(*S*)-(Acetylamino)-α(*S*)-butyl-*N*-[4(*S*)-[(butylamino)carbonyl]-1(*S*)-(cyclohexylmethyl)-2(*S*)-hydroxy-5-methylhexyl]-2-oxo-4(*R*)-phenyl-1-piperidineacetamide (18). To a solution of 13.6 mg (0.021 mmol) of amine **16a** in 0.5 mL of CH_2Cl_2 was added 4.0 μL (0.028 mmol) of triethylamine followed by 2.26 μL (0.024 mmol) of acetic anhydride. The solution was stirred overnight, dissolved in 10 mL of EtOAc, and washed with water (2 × 3 mL) and saturated NaCl solution. The organic phase was dried over $MgSO_4$, filtered, and concentrated. The residue was purified by flash chromatography over silica eluting with 95:5:0.01 $CHCl_3$/MeOH/NH_4OH to give 9.7 mg (0.015 mmol) of acetamide **18** (70% yield) as a glass: characteristic ^1H NMR signals δ 1.89 (s, 3 H), 4.29 (bm, 1 H), 6.02 (t, 1 H), 6.28 (bd, 1 H), 6.95 (bd, 1 H), 7.15–7.38 (m, 5 H); EI exact mass calcd for $C_{38}H_{61}N_4O_5$ 654.47202, found 654.4722.

***N*-Phthaloyl-L-phenylalanine-L-norleucine Methyl Ester (21).** To a solution of 3.0 g (16.5 mmol) of norleucine methyl ester hydrochloride in 20 mL of CH_2Cl_2 was added 2.3 mL (16.5 mmol) of triethylamine. A further 5 mL of CH_2Cl_2 was added to facilitate stirring of the white suspension. To this mixture was added 4.88 g (16.5 mmol) of *N*-phthalylphenylalanine followed by 2.45 g (18.2 mmol) of *N*-hydroxybenzotriazole. The mixture was stirred until a clear golden solution formed. The solution was cooled to 0 °C and treated with 3.48 g (18.2 mmol) of 1-[3-(dimethylamino)-propyl]-3-ethylcarbodiimide hydrochloride. The reaction mixture was then stirred at room temperature overnight. The reaction mixture was diluted with 50 mL of CH_2Cl_2 and washed with 1 × 50 mL of 1 N HCl, water, saturated $NaHCO_3$, water, and saturated NaCl, successively. The organic phase was dried over $MgSO_4$, filtered, and concentrated in vacuo, to give 6.62 g (15.6 mmol) of a white powder (95% yield): ^1H NMR ($CDCl_3$) δ 0.88 (t, 3 H), 1.12–1.25 (m, 3 H), 1.55–1.90 (m, 3 H), 3.55 (m, 2 H), 3.70 (s, 3 H), 4.61 (dd, 1 H), 5.15 (dd, 1 H), 6.63 (d, 1 H), 7.09–7.11 (m, 5 H), 7.65–7.82 (m, 4 H); FABMS *m*/*z* 435 (M^+ + 1).

***N*-Phthaloyl-L-phenylalaninylnorleucine (22).** To 1.0 g (2.37 mmol) of ester **21** in 20 mL of acetone was added 11 mL of water followed by 6 mL of concentrated HCl. The solution was refluxed for 5 h and concentrated to remove acetone and the aqueous solution washed with EtOAc (3 × 20 mL). The organic extracts were extracted with saturated $NaHCO_3$ (2 × 40 mL) and water (1 × 20 mL). The combined aqueous washes were acidified and extracted with EtOAc (3 × 40 mL). The combined organic phases were dried over $MgSO_4$, filtered, and concentrated to give 0.59 g (1.4 mmol) of a white foam (60% yield): ^1H NMR ($CDCl_3$) δ 0.88 (t, 3 H), 1.2–1.4 (m, 4 H), 1.68 (m, 1 H), 1.88 (m, 1 H), 3.53 (m, 2 H), 4.59 (m, 1 H), 5.16 (dd, 1 H), 6.68 (d, 1 H), 7.08–7.20 (m, 5 H), 7.65–7.80 (m, 4 H); FABMS *m*/*z* 409 (M^+ + 1).

4(*S*)-Butyl-3-[2(*S*)-(1,3-dihydro-1,3-dioxo-2*H*-isoindol-2-yl)-1-oxo-3-phenylpropyl]-5-oxazolidinone (23). A solution of 0.95 g (2.3 mmol) of acid **22** in 55 mL of benzene was heated under a Dean–Stark trap with 0.87 g of paraformaldehyde and 0.05 g of *p*-toluenesulfonic acid for 6 h. The reaction mixture was concentrated in vacuo and the residue dissolved in 50 mL of EtOAc. The solution was washed with saturated $NaHCO_3$ (2 × 15 mL) and saturated NaCl (1 × 15 mL). The solution was dried over $MgSO_4$, filtered, and concentrated in vacuo. The residue was purified by vacuum filtration through a pad of silica gel to remove baseline contaminants. Oxazolidinone **23** was recovered as a foam: 0.61 g (1.4 mmol), 63% yield, ^1H NMR ($CDCl_3$) δ 0.97 (3 H, t), 1.1–1.4 (4 H, m), 1.6–2.02 (m, 4 H), 4.62 (m, 1 H), 5.02 (dd, 2 H, 5.28 (m, 1 H), 7.18 (m, 5 H), 7.80 (m, 4 H); FABMS *m*/*z* 421 (M^+ + 1).

4(*S*)-Butyl-4(*S*)-(1,3-dihydro-1,3-dioxo-2*H*-isoindol-2-yl)-1,3,4,5-tetrahydro-3-oxo-2*H*-2-benzazepine-2-acetic Acid (24). A solution of 0.61 g (1.46 mmol) of oxazolidinone **23** in 2 mL of dry CH_2Cl_2 was added to 2.0 mL of triflic acid at room temperature. The reaction mixture turned black and was stirred overnight. The solution was diluted with 30 mL of CH_2Cl_2 and washed with water (2 × 20 mL) and brine (1 × 20 mL). The organic phase was dried over $MgSO_4$, filtered, and concentrated to give 0.59 g (1.4 mmol) of **24** as light brown crystals. TLC analysis of this product indicated that it consisted of a single UV-active homogeneous product, R_f = 0.75 (SiO_2, 10:90:1 MeOH/EtOAc/HOAc) (96% yield): ^{1}H NMR δ 0.81 (3 H, t), 1.02–1.25 (4 H, m), 1.88 (m, 1 H), 2.07 (m, 1 H), 3.08 (dd, 1 H), 4.05 (dd, 1 H), 4.47 (d, 1 H), 4.79 (d, 1 H), 5.20 (m, 2 H), 7.14–7.35 (m, 4 H), 7.73 (m, 2 H), 7.89 (m, 2 H), COOH, not observed; FABMS *m/z* 421 (M^+ + 1) calcd for $C_{24}H_{24}N_2O_5$.

4(*S*)-Butyl-*N*-[4(*S*)-[(butylamino)carbonyl]-1(*S*)-(cyclohexylmethyl)-2(*S*)-hydroxy-5-methylhexyl]-4(*S*)-(1,3-dihydro-1,3-dioxo-2*H*-isoindol-2-yl)-1,3,4,5-tetrahydro-3-oxo-2*H*-2-benzazepine-2-acetamide (25). A solution of 0.18 g (0.42 mmol) of acid **24** and 0.137 g (0.42 mmol) of the amine *N*-*n*-butyl-(2*S*,4*S*,5*S*)-5-amino-6-cyclohexyl-4-hydroxy-2-isopropylhexanamide were dissolved in 1 mL of CH_2Cl_2 and treated with 0.062 g (0.46 mmol) of *N*-hydroxybenzotriazole followed by 0.088 g (0.46 mmol) of 1-[3-(dimethylamino)propyl]-3-ethylcarbodiimide hydrochloride. The reaction mixture was stirred overnight and subsequently concentrated in vacuo. The residue was dissolved in 30 mL of EtOAc and washed with (2 × 20 mL) 1 N HCl, saturated $NaHCO_3$, water, and brine. The organic phase was dried over $MgSO_4$, filtered, and concentrated in vacuo. The residue (0.29 g) was purified by flash chromatography over silica eluting with 4% MeOH/CH_2Cl_2 to give 0.24 g of a beige foam (78% yield): characteristic ^{1}H NMR ($CDCl_3$) signals δ 0.78 (t, 3 H), 0.85–0.92 (m, 9 H), 2.05 (dt, 1 H), 3.0–3.2 (m, 2 H), 3.27 (m, 1 H), 4.15 (d, 1 H), 4.90 (d, 1 H), 5.08 (dd, 1 H), 5.37 (dd, 1 H), 5.69 (t, 1 H), 6.79 (d, 1 H), 7.25–7.67 (m, 4 H), 7.73–7.91 (m, 4 H); FABMS *m/z* 729 (M^+ + 1); EI exact mass calcd for $C_{43}H_{60}N_4O_6$ 728.4513, found 728.4511.

4(*S*)-Amino-α(*S*)-butyl-*N*-[4(*S*)-[(butylamino)carbonyl]-1(*S*)-(cyclohexylmethyl)-2(*S*)-hydroxy-5-methylhexyl]-1,3,4,5-tetrahydro-3-oxo-2*H*-2-benzazepine-2-acetamide (26). A solution of 118 mg (0.16 mmol) of peptide **25** in 0.65 mL of EtOH was treated with 16 μL (0.32 mmol) of hydrazine hydrate. The reaction mixture was heated under reflux under N_2 for 1 h and the residue dissolved in 10 mL of CH_2Cl_2. A precipitate of phthaloyl hydrazide was removed by filtration and the filtrate was concentrated in vacuo. The residue was purified by flash chromatography over silica gel eluting with 90:9:1 $CHCl_3$/MeOH/NH_4OH to give rise to 0.091 g (0.15 mmol) of amine **26** (94% yield) as a foam: characteristic ^{1}H NMR ($CDCl_3$) signals δ 2.98 (dd, 1 H), 3.11–3.35 (m, 3 H), 3.42–3.60 (m, 2 H), 4.25 (d, 1 H), 4.35 (dd, 1 H), 4.88 (d, 1 H), 4.96 (dd, 1 H), 5.80 (t, 1 H), 6.04 (d, 1 H), 7.05–7.26 (m, 4 H); FABMS *m/z* 599 (M^+ + 1); EI exact mass calcd for $C_{35}H_{58}N_4O_4$ 598.4458, found 598.4439.

4(*S*)-Butyl-4(*S*)-[(*tert*-butyloxycarbonyl)amino]-*N*-[4(*S*)-[(butylamino)carbonyl]-1(*S*)-(cyclohexylmethyl)-2(*S*)-hydroxy-5-methylhexyl]-1,3,4,5-tetrahydro-3-oxo-2*H*-2-benzazepine-2-acetamide (27). To a solution of 0.041 g (0.068 mmol) of amine **26** in 0.25 mL of CH_2Cl_2 was added 9.5 μL (0.068 mmol) of triethylamine followed by 16 mg (0.075 mmol) of di-*tert*-butyl dicarbonate. The solution was stirred overnight and concentrated in vacuo. The residue was purified by flash chromatography over silica eluting with 96:4:0.5 $CHCl_3$/MeOH/NH_4OH to give a single product (**27**) as a foam (0.041 g, 0.59 mmol, 86% yield): characteristic ^{1}H NMR ($CDCl_3$) signals δ 1.45 (s, 9 H), 2.05 (m, 1 H), 3.02 (dd, 1 H), 3.19 (m, 1 H), 3.31 (m, 1 H), 3.39–3.55 (m, 2 H), 3.73 (m, 1 H), 3.91 (fd, 1 H), 4.23 (d, 1 H), 4.92 (m, 2 H), 5.15 (m, 1 H), 5.70 (t, 1 H), 5.85 (bm, 2 H), 7.02–7.25 (m, 4 H); FABMS *m/z* 699 (M^+ + 1); EI exact mass, calcd 698.4982, found 698.4984. Anal. ($C_{40}H_{66}N_4O_6$) C, H, N.

4(*S*)-(Acetylamino)-α(*S*)-butyl-*N*-[4(*S*)-[(butylamino)carbonyl]-1(*S*)-(cyclohexylmethyl)-2(*S*)-hydroxy-5-methylhexyl]-1,3,4,5-tetrahydro-3-oxo-2*H*-2-benzazepine-2-acetamide (28). Acetic anhydride (6.6 μL, 0.07 mmol) was added at room temperature to a solution of 38 mg (0.06 mmol) of amine **26** in 0.35 mL of CH_2Cl_2. After 1 h the reaction mixture was diluted with 10 mL of CH_2Cl_2 and washed with 5 mL of water. The organic phase was dried over $MgSO_4$, filtered, and concentrated in vacuo. The residue was purified by flash chromatography over silica eluting with 10% MeOH/CH_2Cl_2 and gave rise to 38 mg (0.06 mmol) of acetamide **28** (100% yield) as a foam: characteristic ^{1}H NMR ($CDCl_3$) signals δ 2.05 (s, 3 H), 2.98 (dd, 1 H), 2.18 (m, 1 H), 2.30 (m, 1 H), 3.90 (d, 1 H), 4.25 (d, 1 H), 4.91 (d, 1 H), 5.98 (m, 1 H), 5.37 (m, 1 H), 5.68 (t, 1 H), 5.90 (d, 1 H), 6.91 (d, 1 H), 7.04–7.22 (m, 4 H); FABMS *m/z* 641 (M^+ + 1); EI exact mass calcd for $C_{37}H_{60}N_4O_5$ 628.4564, found 628.4534.

***N*-[1-[[[4(*S*)-[(Butylamino)carbonyl]-1(*S*)-(cyclohexylmethyl)-2(*S*)-hydroxy-5-methylhexyl]amino]carbonyl]-pentyl]-1,3-dihydro-1,3-dioxo-α(*S*)-(phenylmethyl)-2*H*-isoindole-2-acetamide (29).** A solution of 0.15 g (0.37 mmol) of **22** in 0.5 mL of CH_2Cl_2 was added to a 0 °C solution of 0.12 g (0.37 mmol) of *N*-*n*-butyl-(2*S*,4*S*,5*S*)-5-amino-6-cyclohexyl-4-hydroxy-2-isopropylhexanamide in 1 mL of CH_2Cl_2 followed by 55 mg (0.41 mmol) of *N*-hydroxybenzotriazole and 78 mg (0.41 mmol) of DCC. The solution was allowed to warm to room temperature and stirred overnight. The reaction mixture was concentrated in vacuo and the residue was subsequently redissolved in EtOAc (25 mL) and washed with 1 N HCL (2 × 5 mL), saturated $NaHCO_3$ (1 × 5 mL), water (1 × 5 mL), and brine (1 × 5 mL). The organic phase was dried over $MgSO_4$, filtered, and concentrated. The residue was purified by MPLC silica Lobar A column eluting with 2.5% MeOH/CH_2Cl_2 to give rise to 91 mg (0.12 mmol) of a white foam (34% yield): mp 194–196 °C; characteristic ^{1}H NMR ($CDCl_3$) signals δ 0.75–0.95 (m, 12 H), 2.00 (dt, 1 H), 3.10–3.33 (m, 2 H), 3.50 (m, 3 H), 3.87 (bm, 1 H), 3.92 (d, 1 H), 4.36 (dd, 1 H), 5.13 (dd, 1 H), 5.93 (t, 1 H), 6.42 (d, 1 H), 6.60 (d, 1 H) 7.10–7.23 (m, 5 H), 7.69–7.80 (m, 4 H); FABMS *m/z* 717 (M^+ + 1).

L-Phenylalanyl-*N*-[4(*S*)-[(butylamino)carbonyl]-1(*S*)-(cyclohexylmethyl)-2(*S*)-hydroxy-5-methylhexyl]-L-norleucinamide (30). To a suspension of 76 mg (0.106 mmol) of peptide **29** in 1 mL of EtOH was added 10 μL (0.21 mmol) of hydrazine hydrate. The mixture was reflux ed for 3 h. The reaction mixture was concentrated in vacuo, the residue redissolved in $CHCl_3$ and filtered, and the filtrate concentrated in vacuo to give 42 mg (0.07 mmol) of a white powder (68% yield): characteristic ^{1}H NMR ($CDCl_3$) signals δ 0.8–0.95 (m, 12 H), 2.03 (dt, 1 H), 2.75 (dd, 1 H), 3.18–3.32 (m, 3 H), 3.60 (m, 2 H), 3.88 (m, 1 H), 4.30 (dd, 1 H), 6.12 (t, 1 H), 6.51 (d, 1 H), 7.19–7.37 (m, 5 H), 7.83 (d, 1 H); FABMS *m/z* 587 (M^+ + 1).

***N*-[(1,1-Dimethylethoxy)carbonyl]-L-phenylalanyl-*N*-[4(*S*)-[(butylamino)carbonyl]-1(*S*)-(cyclohexylmethyl)-2(*S*)-hydroxy-5-methylhexyl]-L-norleucinamide (31).** The procedure was as for **27**. Purification was by trituration with CH_2Cl_2: 95% yield; characteristic ^{1}H NMR (CD_3OD) signals δ 0.85–0.98 (m, 12 H), 1.33 (s, 9 H), 2.17 (dt, 1 H), 2.81 (dd, 1 H), 3.38 (d, 1 H), 3.89 (m, 1 H), 4.30 (m, 2 H), 7.18–7.32 (m, 5 H), 7.87 (t, 1 H).

***N*-Acetyl-L-phenylalanyl-*N*-[4(*S*)-[(butylamino)carbonyl]-1(*S*)-(cyclohexylmethyl)-2(*S*)-hydroxy-5-methylhexyl]-L-norleucinamide (32).** The procedure was as for **28**. Purification was by trituration with CH_2Cl_2: 50% yield; characteristic ^{1}H NMR (DMSO-d_6) signals δ 0.78–0.91 (m, 12 H), 1.72 (s, 3 H), 2.09 (m, 1 H), 2.71 (dd, 1 H), 3.72 (bm, 1 H), 4.22 (m, 1 H), 4.50 (m, 2 H), 7.15–7.35 (m, 5 H), 7.65 (t, 1 H), 8.10 (bd, 2 H); FABMS *m/z* 629 (M^+ + 1).

Biological Methods. Human plasma renin inhibition was determined by radioimmunoassay for angiotensin I, as described by Haber et al.[32] and detailed by Poe et al.[33] using a commercial kit (Clinical Assays, Cambridge, MA) at pH 7.4 (phosphate), 37 °C. Plasma inhibition values (IC_{50}) were the mean of three determinations.

(32) Haber, E.; Koerner, T.; Page, L. B.; Kliman, B.; Purdnoe, A. J. Application of a Radioimmunoassay for Angiotensin I to the Physiological Measurement of Plasma Renin Activity in Normal Human Subjects. *J. Clin. Endocrinol.* **1969**, *29*, 1349–1355.

(33) Poe, M.; Wu, J. K.; Florance, J. R.; Rodkey, J. A.; Bennett, C. D.; Hoogsteen, K. J. Purification and Properties of Renin and γ-Renin from the Mouse Submaxilliary Gland. *J. Biol. Chem.* **1983**, *258*, 2209–2216.

Acknowledgment. We thank Mr. R. Brown and Dr. C. Caldwell for spectroscopic and analytical support.

Registry No. **2**, 4160-80-9; **3**, 61949-75-5; 4, 138571-09-2; **5**, 138571-10-5; **6**, 131906-19-9; **7a**, 138571-11-6; **7b**, 138571-30-9; **8a**, 138571-12-7; **8b**, 138662-92-7; **9a**, 138571-13-8; **9b**, 138662-93-8; 11, 138605-19-3; **12a**, 138605-20-6; **12b**, 138571-31-0; **14a**, 138605-21-7; **15a**, 138571-14-9; **15b**, 138662-94-9; **16a**, 138571-15-0; **16b**, 138662-95-0; **17a**, 138571-16-1; **17b**, 138662-96-1; 18, 138571-17-2; **21**, 138571-18-3; **22**, 138571-19-4; **23**, 138571-20-7; **24**, 138571-21-8; **25**, 138571-22-9; **26**, 138571-23-0; **27**, 138571-24-1; **28**, 138571-25-2; **29**, 138571-26-3; **30**, 138571-27-4; **31**, 138571-28-5; **32**, 138571-29-6; $PhCH_2Br$, 100-39-0; $HOCH_2CH_2OH$, 107-21-1; H-Nle-OBu-*t*, 15911-73-6; N-Nle-OMe·HCl, 3844-54-0; 3-phenylglutaric acid, 4165-96-2; (*S*)-(−)-4-benzyl-2-oxazolidinone, 90719-32-7; *N*-butyl (2*S*,4*S*,5*S*)-5-amino-6-cyclohexyl-4-hydroxy-2-isopropylhexanamide, 105852-64-0; *N*-phthalylphenylalanine, 5123-55-7; paraformaldehyde, 30525-89-4; renin, 9015-94-5.

Supplementary Material Available: Coordinates of all molecular model conformations discussed in this work are available (76 pages). Ordering information is given on any current masthead page.